X-ray Diffraction

- Basic aspects of x-ray crystallography and powder diffraction

- Diffraction from nanocrystalline materials

Paolo.Scardi@unitn.it

PART I

Diffraction from nanocrystalline materials:
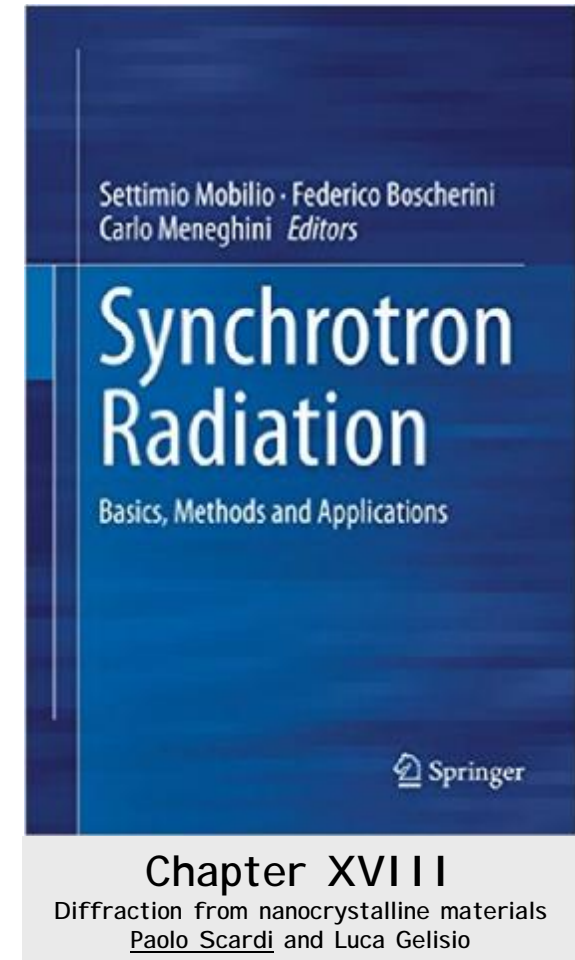why using synchrotron radiation?

PART II

Reciprocal space vs direct
space methods

PART III

Selected case studies:
highly deformed metals,
and nanocrystalline catalyst

PART IV

Total Scattering methods

Settimio Mobilio · Federico Boscherini
Carlo Meneghini *Editors*

Synchrotron Radiation

Basics, Methods and Applications

Springer

Chapter XVIII
Diffraction from nanocrystalline materials
Paolo Scardi and Luca Gelisio
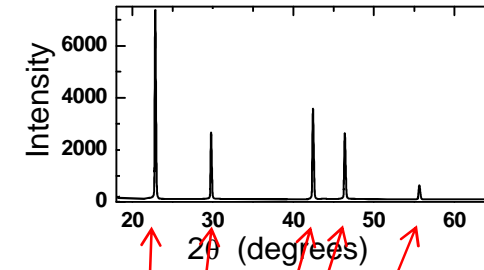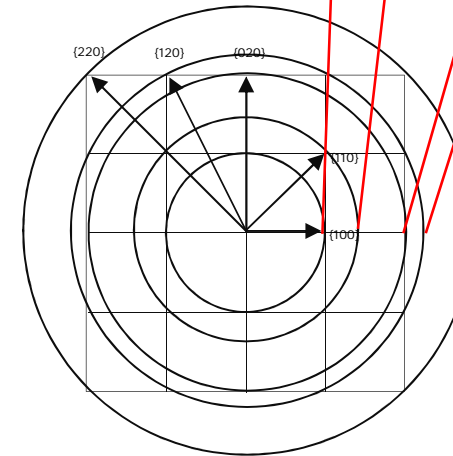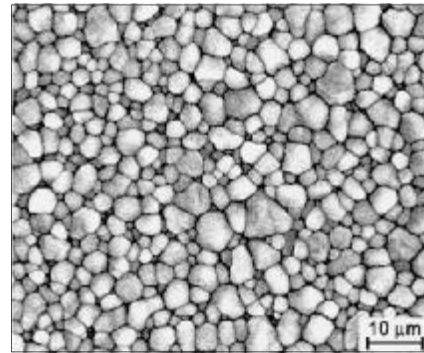
SYNCHROTRON RADIATION X-RAY DIFFRACTION

main applications of (powder /polycrystalline material) diffraction

- Crystal structure determination: structure solution and refinement.

- Line Profile Analysis (LPA): crystalline domain size/shape, lattice defect analysis – nanocrystalline materials

- Phase Identification (Search-Match procedures): pure crystalline phases or mixtures
- Quantitative Phase Analysis (QPA): crystalline and amorphous phases

- Texture Analysis (TA): determination of preferred orientations
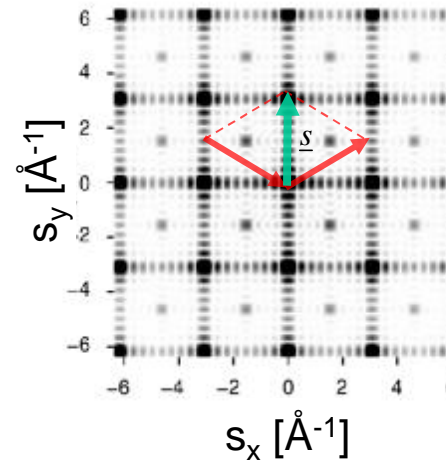- X-ray Residual Stress Analysis (XRSA): measurement of strain field / elastic behaviour

DIFFRACTION PATTERN FROM A POLYCRYSTALLINE

powder
(bulk polycrystalline)
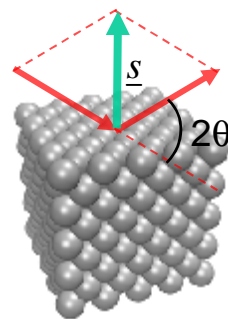
$$s = Q/2\pi = 2\sin\theta / \lambda$$

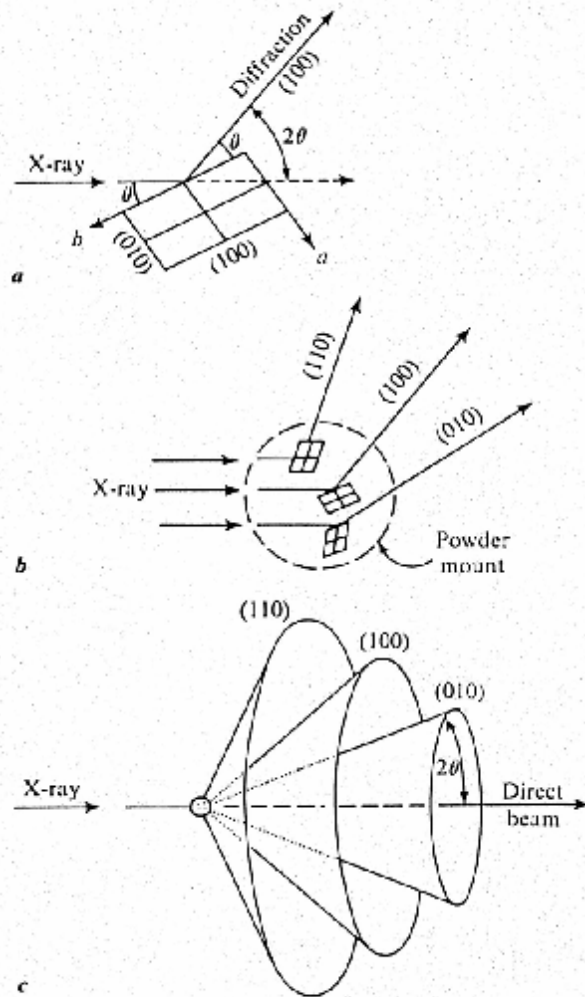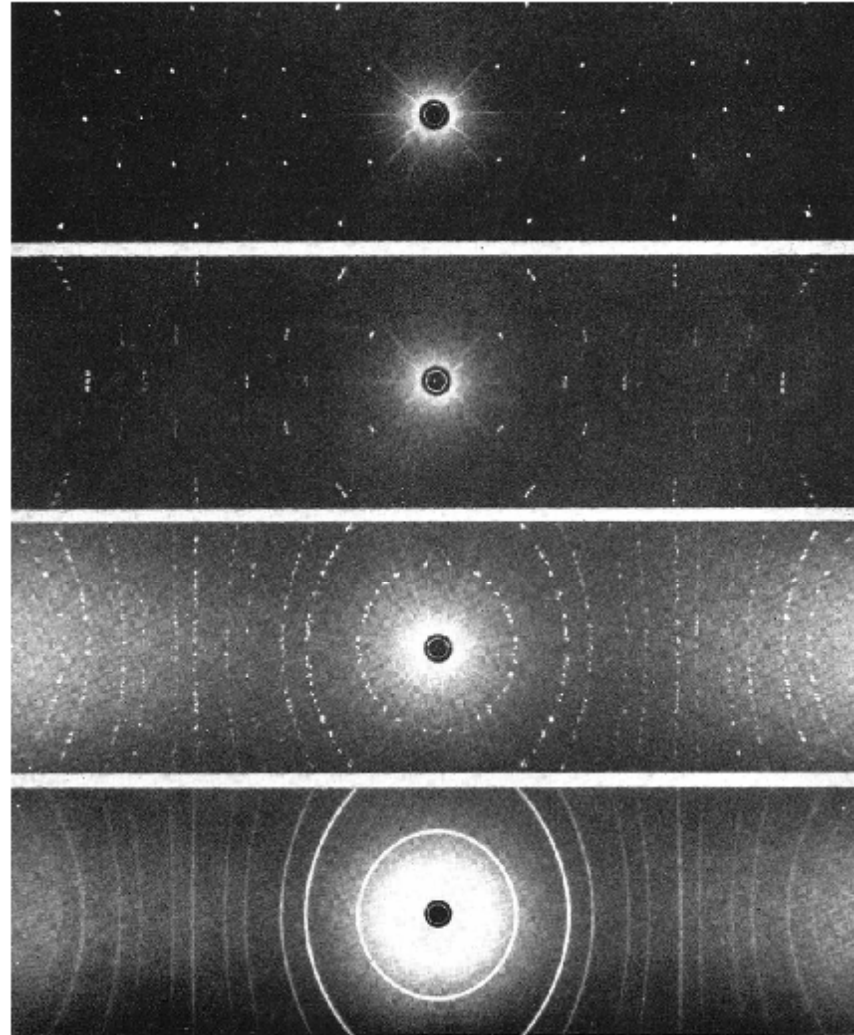## from single-crystal to powder diffraction

FIGURE 10.11 Diffraction of monochromatic x-rays from (a) a single crystal and (b) an aggregate of small mineral fragments. (c) Diffraction cones produced by the powder method.


(*From top to bottom*). Fig. 197; Single-crystal rotation photograph of fluorite [100] vertical: Fig. 198; Single-crystal rotation photograph of fluorite [100] 2° to vertical: Fig. 199; X-ray photograph of five randomly oriented crystals of fluorite; Fig. 200; Powder photograph of fluorite.
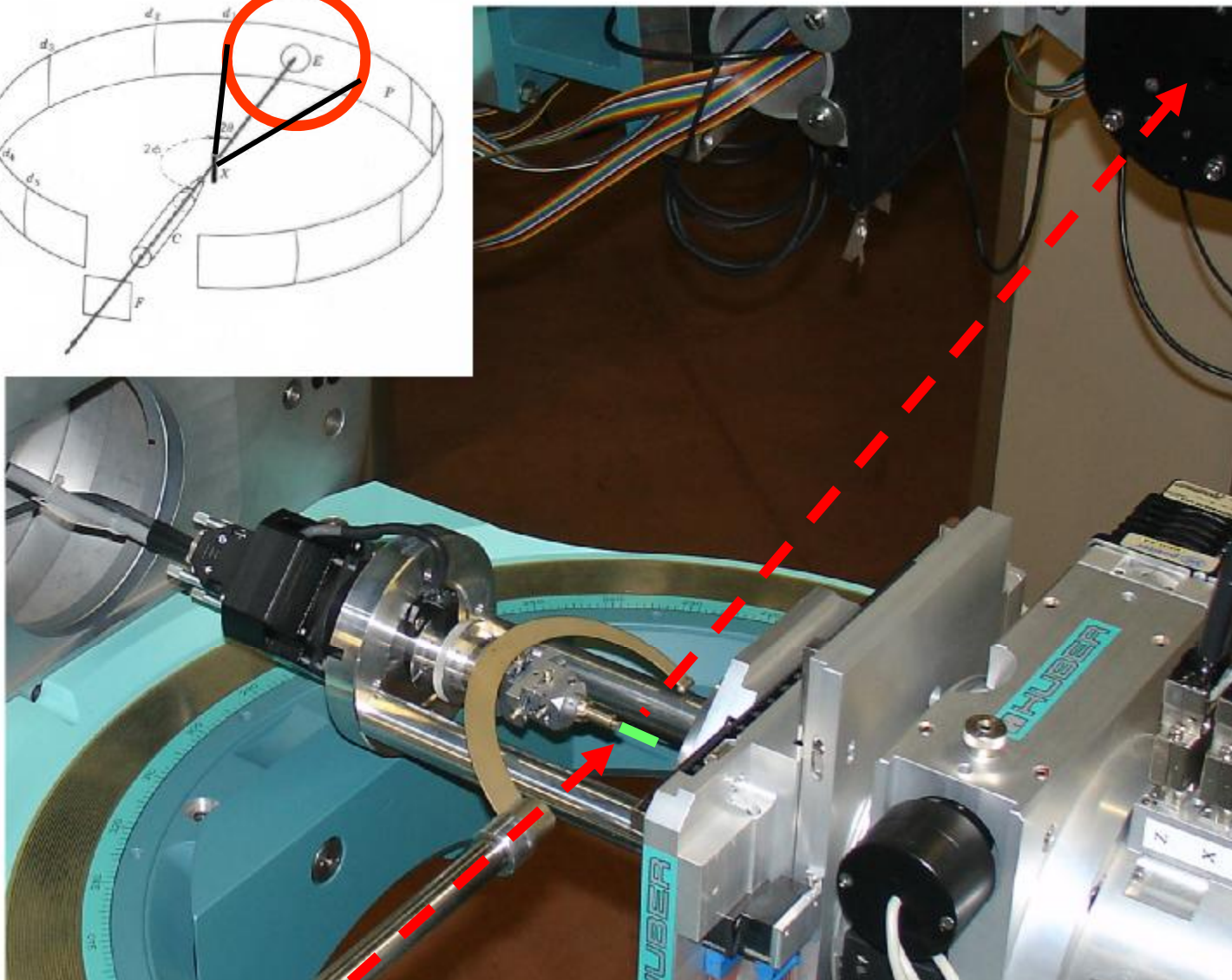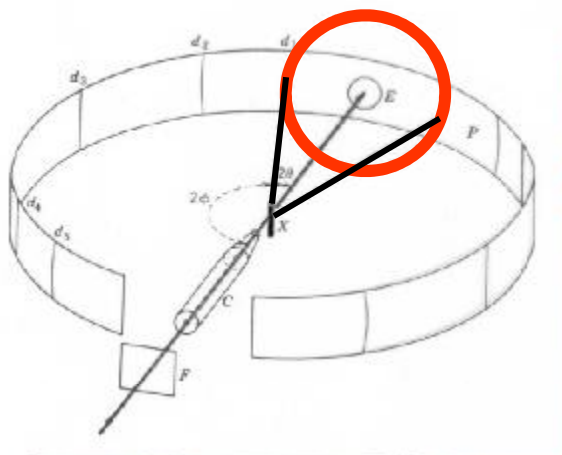
SYNCHROTRON RADIATION X-RAY DIFFRACTION

Powder diffraction 'elective' geometry: Debye-Scherrer (1918)
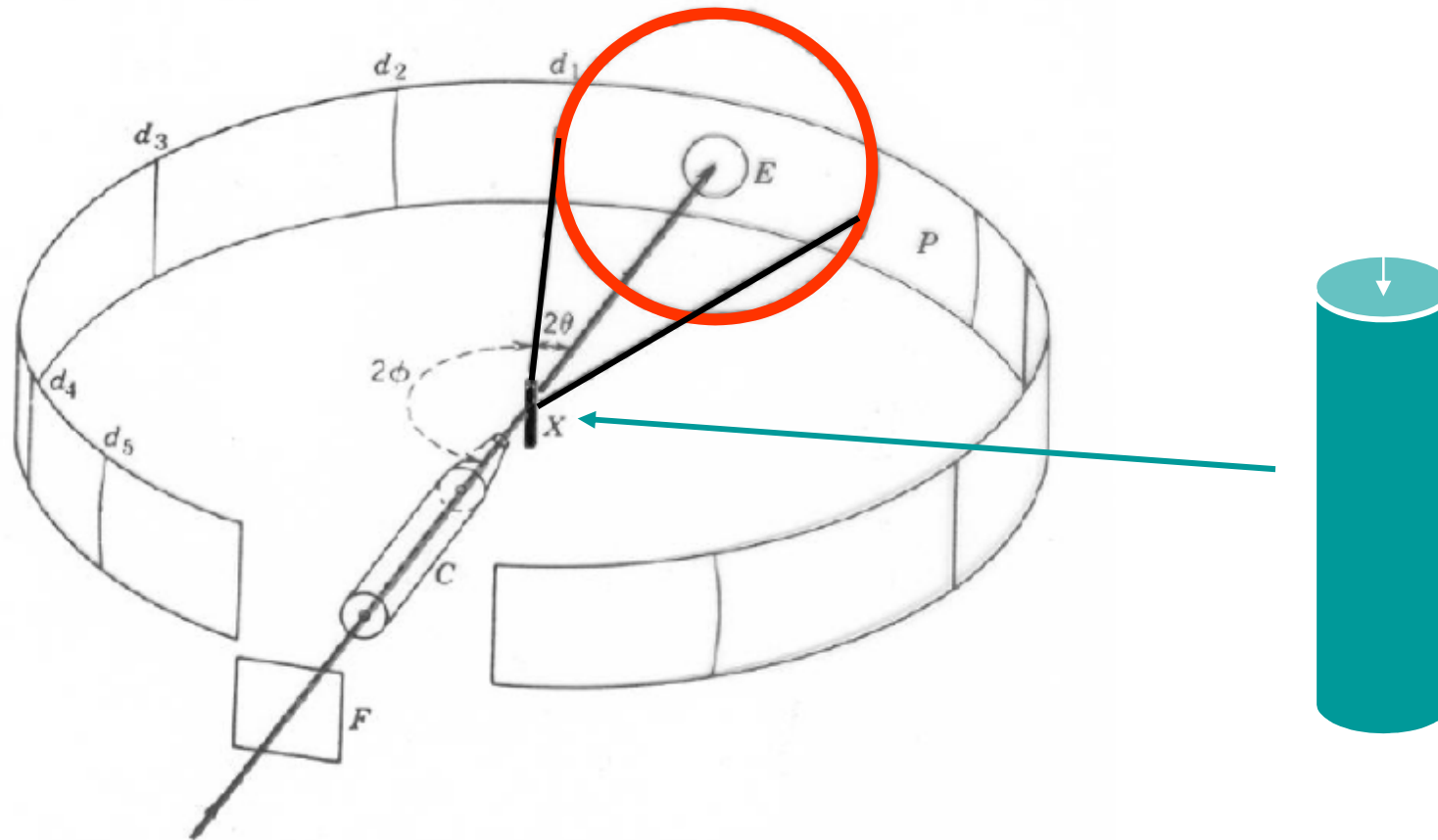
SYNCHROTRON RADIATION X-RAY DIFFRACTION
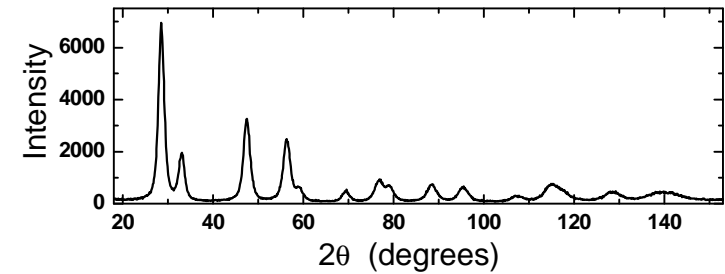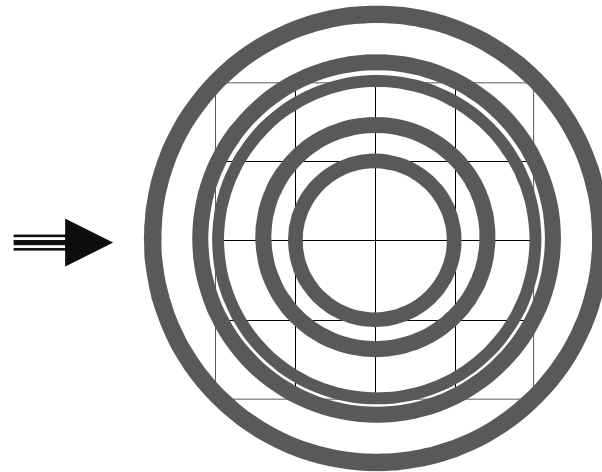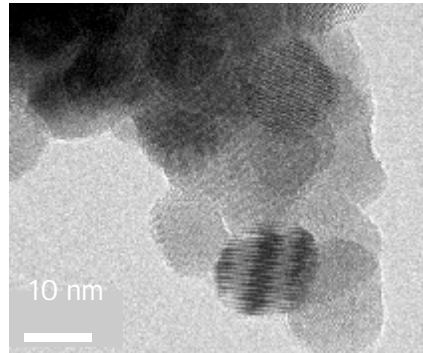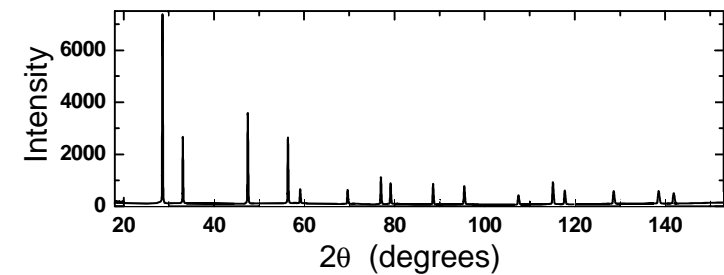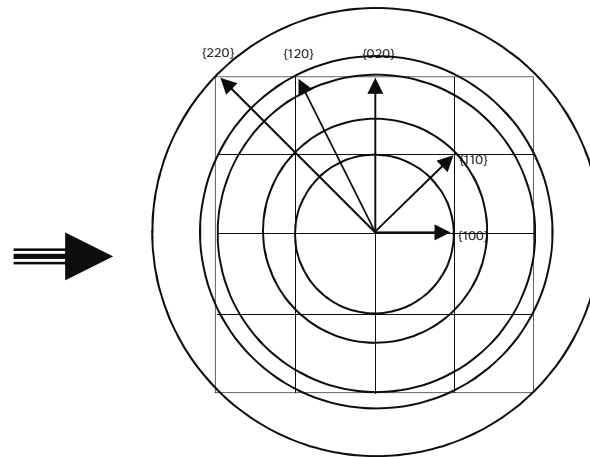## parallel beam, Debye Sherrer geometry of MCX (ELETTRA)
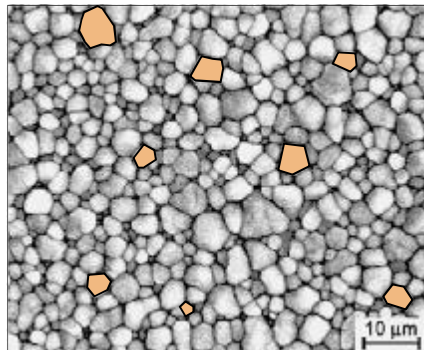
DIFFRACTION PATTERN FROM A POLYCRYSTALLINE

peaks from nanocrystals are broad: why using SR ???

nanocrystalline
powder

powder
(bulk polycrystalline)

SYNCHROTRON RADIATION X-RAY DIFFRACTION

• high brillance: better counting statistics / shorter data collection time / fast kinetics, in situ, in operando studies

Lab instrument: ~80.000s

9-crystal analyzer: 1.500s ! (x100 counts)

$$\frac{counts \cdot N° \ of \ peaks}{time} = 1$$

=25.000

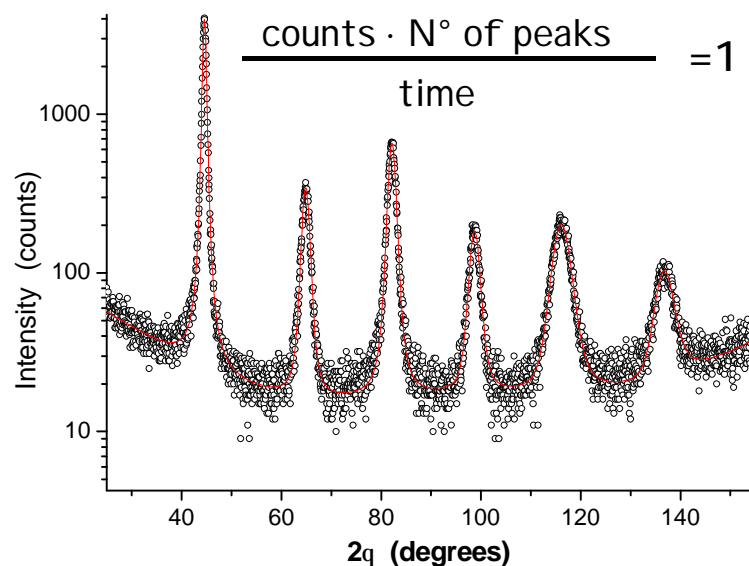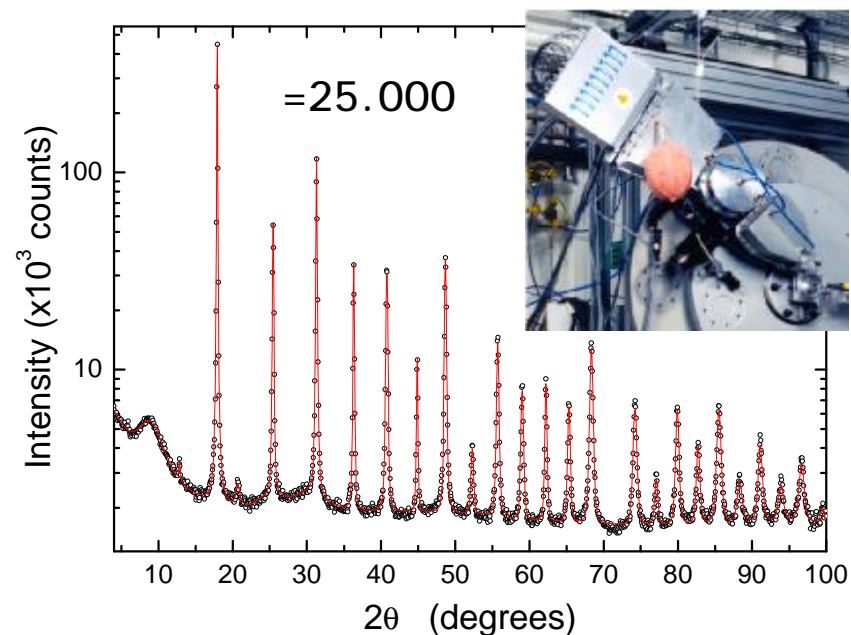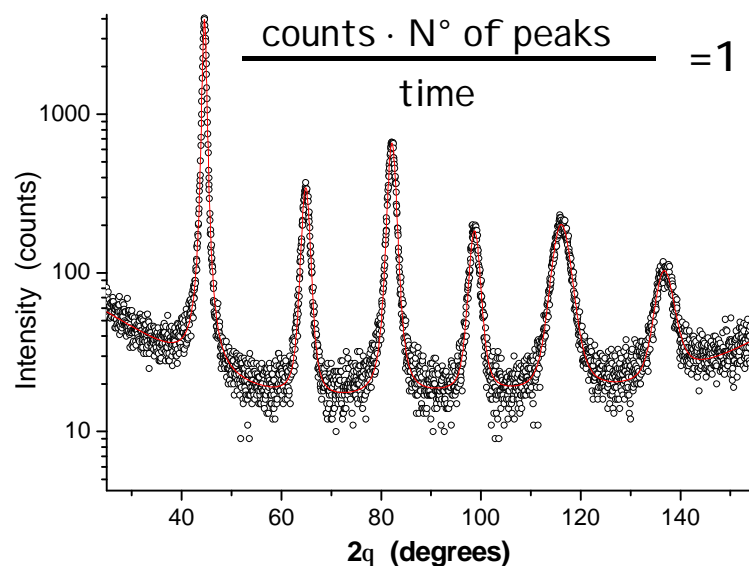CuKα λ=0.15406 nm   ESRF ID31 (now ID22) λ=0.0632 nm

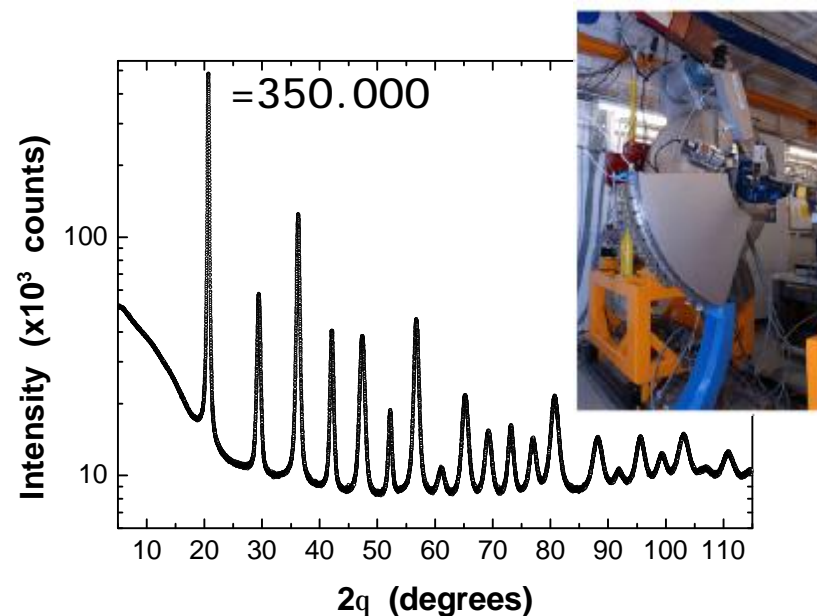iron powder (ball milled)

SYNCHROTRON RADIATION X-RAY DIFFRACTION

- high brillance: better counting statistics / shorter data collection time / fast kinetics, in situ, in operando studies

Lab instrument: ~80.000s

Mythen detector: 100 s !! (x100 counts)

$$\frac{counts \cdot N° \text{ of peaks}}{time} = 1$$
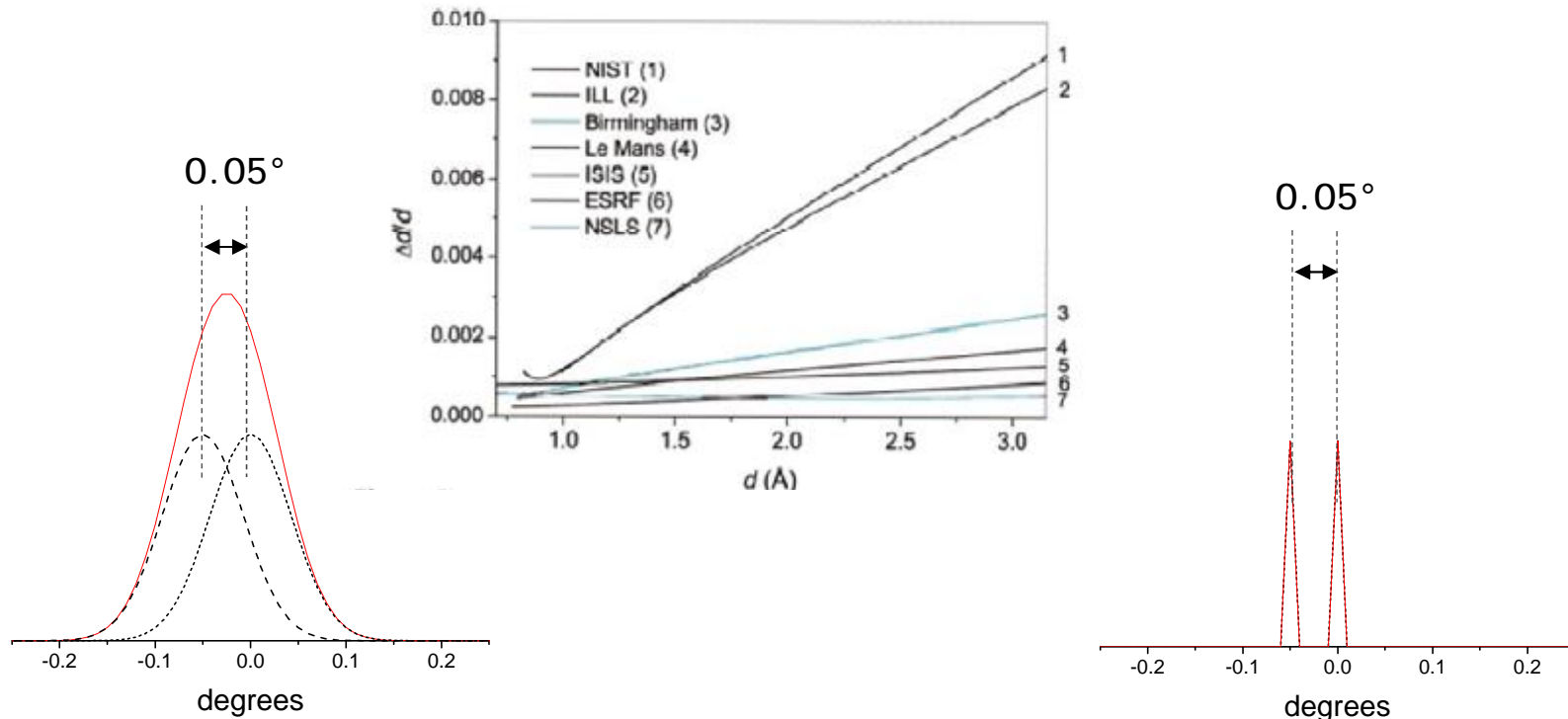
=350.000

CuKα λ=0.15406 nm   PSI MS-X04SA λ=0.072929 nm

iron powder (ball milled)

SYNCHROTRON RADIATION X-RAY DIFFRACTION

- narrow instrumental profile: control of instrumental profile; high resolution and accuracy in measuring peak position, intensity and profile width/shape
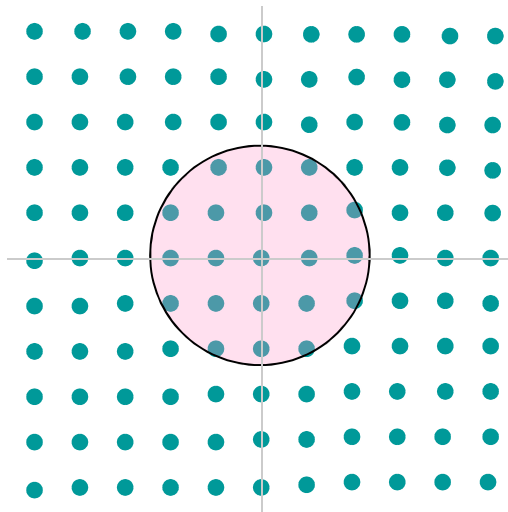

0.05°

0.05°

degrees

degrees

Lab instrument:
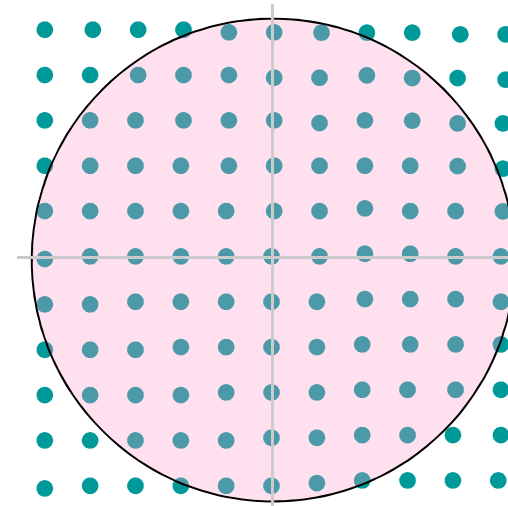## FWHM≈0.05-0.1°

ID31 @ESRF:
FWHM≈0.003-0.004°

SYNCHROTRON RADIATION X-RAY DIFFRACTION

- extending the accessible region of reciprocal space well beyond what traditional lab instruments can make

$$\lambda_1 \qquad\qquad \lambda_2 < \lambda_1$$

SYNCHROTRON RADIATION X-RAY DIFFRACTION

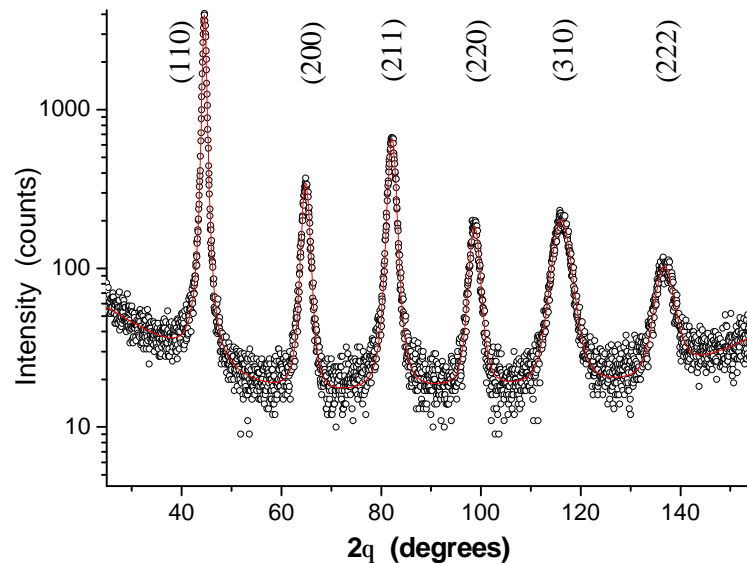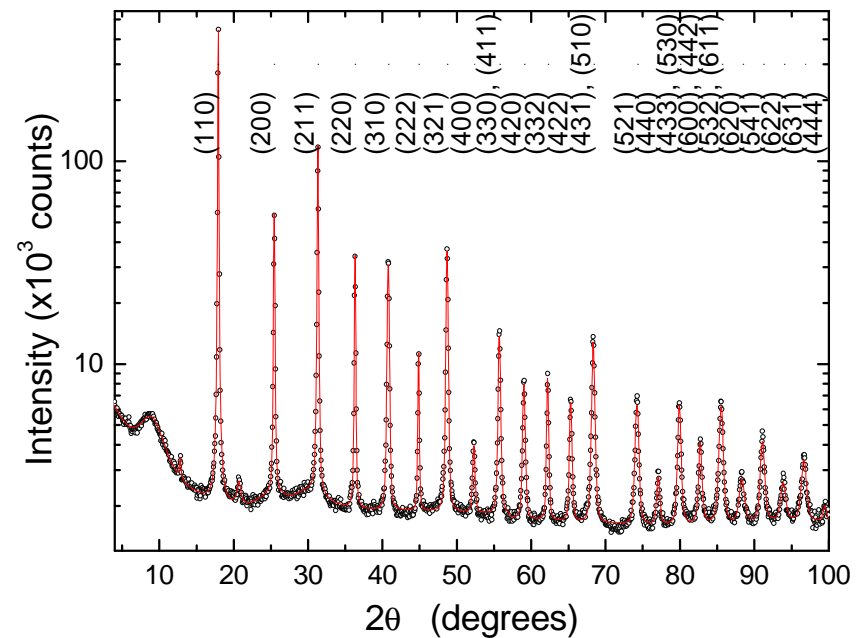- extending the accessible region of reciprocal space well beyond what traditional lab instruments can make

Lab instrument: ~80.000s
: 6 peaks

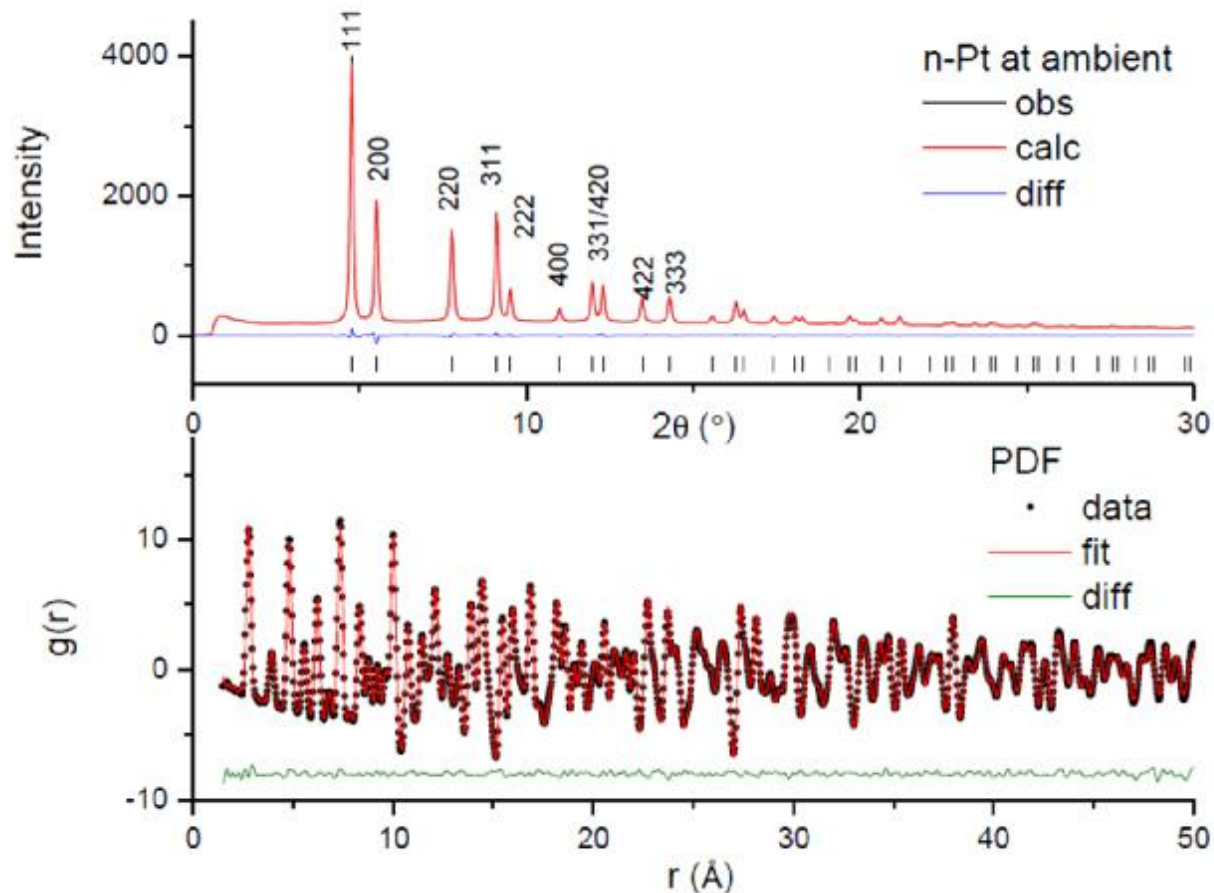9-crystal analyzer: 1.500s! (x100 counts)
: 28 peaks

CuKα λ=0.15406 nm

ESRF ID31 λ=0.0632 nm

SYNCHROTRON RADIATION X-RAY DIFFRACTION

- extending the accessible region of reciprocal space well beyond what traditional lab instruments can make: PDF analysis

High-pressure pair distribution function (PDF) measurement of nano Pt (50 nm) at 12.5 GPa in Methanol:Ethanol = 4:1. Focused X-ray beam, **66.054 keV**, Brookhaven National Laboratory.   Hong et al., Nat. Sci. Reports 6, 21434 (2016)

SYNCHROTRON RADIATION X-RAY DIFFRACTION

• extending the accessible region of reciprocal space well beyond what traditional lab instruments can make: PDF analysis
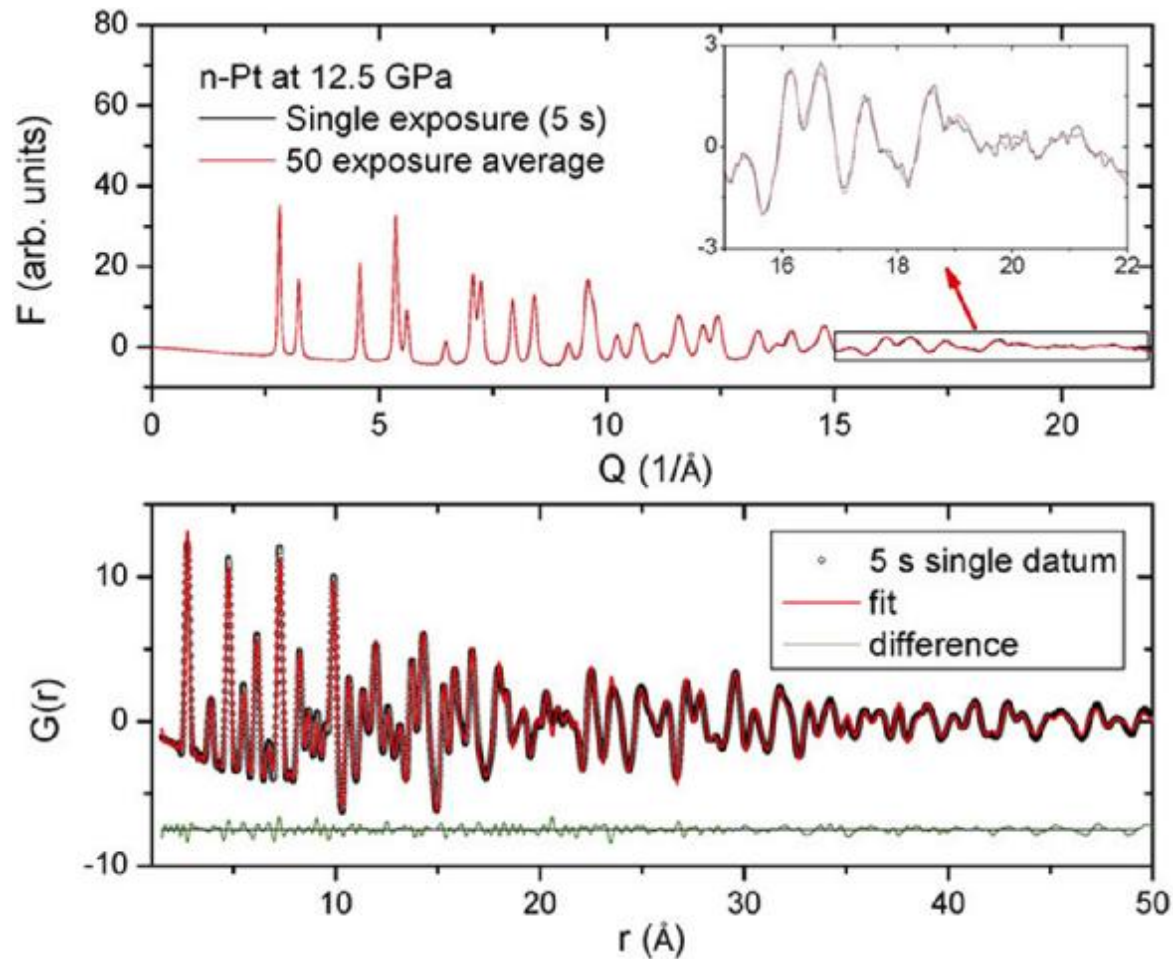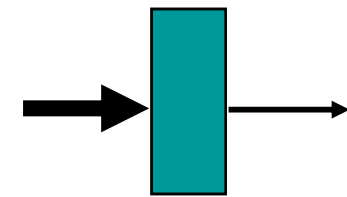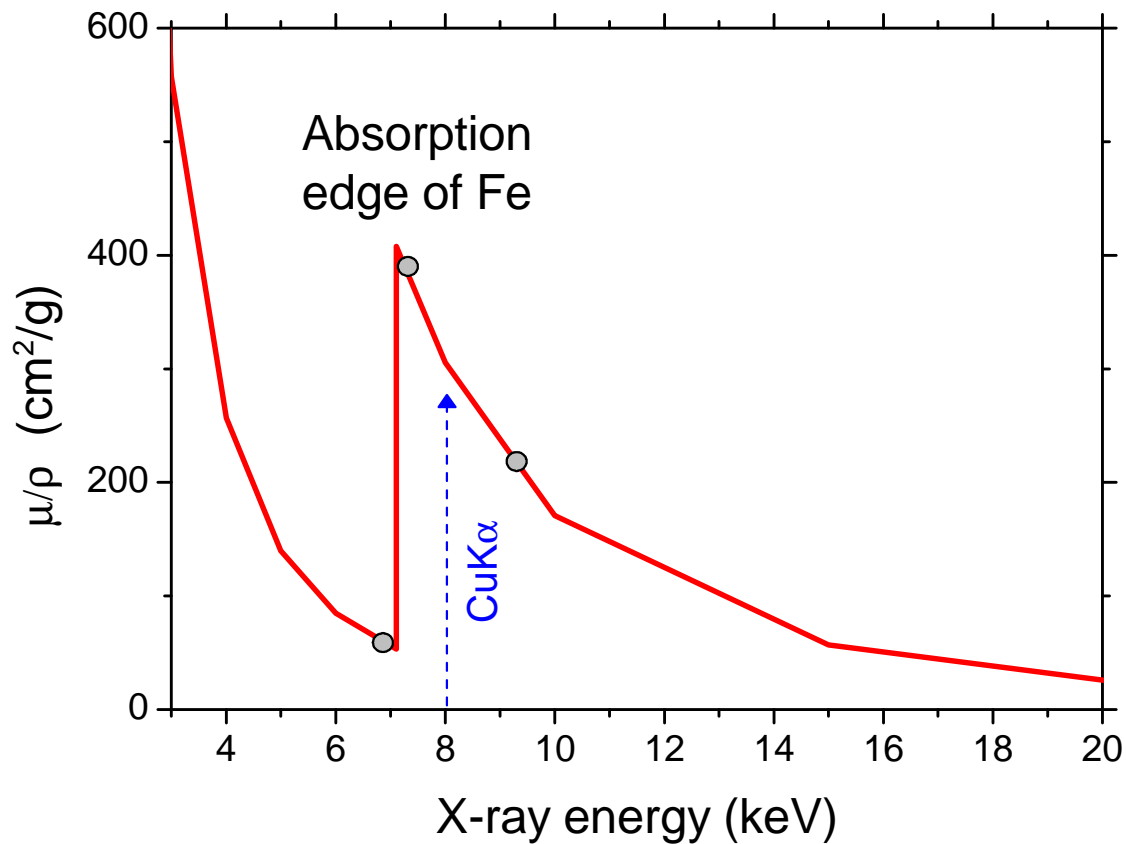

High-pressure pair distribution function (PDF) measurement of nano Pt (50 nm) at 12.5 GPa in Methanol:Ethanol = 4:1. Focused X-ray beam, 66.054 keV, Brookhaven National Laboratory.   Hong et al., Nat. Sci. Reports 6, 21434 (2016)
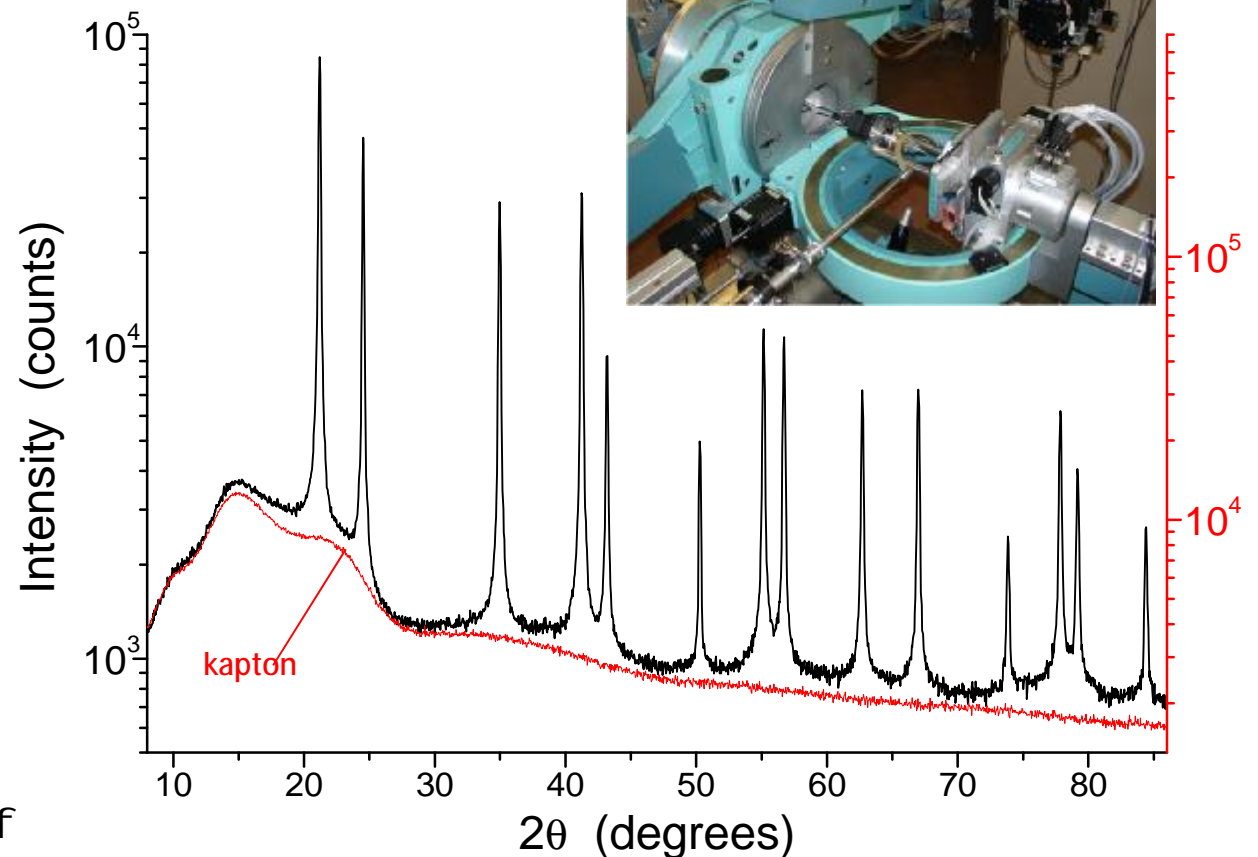
SYNCHROTRON RADIATION X-RAY DIFFRACTION

- tuning energy according to adsorption edges for, e.g.:
  resonant scattering, in depth measurements (property gradients)

$$I = I_0 e^{-\left(\frac{m}{r}\right)rt}$$

SYNCHROTRON RADIATION X-RAY DIFFRACTION

- tuning energy according to adsorption edges for, e.g.:
  resonant scattering, in depth measurements (property gradients);
  control fluorescence emission and *absorption*

MCX beamline (Elettra), 15 keV

Negligible absorption: $\mu = 2.71$ cm^{-1} à $\mu R \approx 0.07$

kapton

Special thanks to: M. Abdellatief
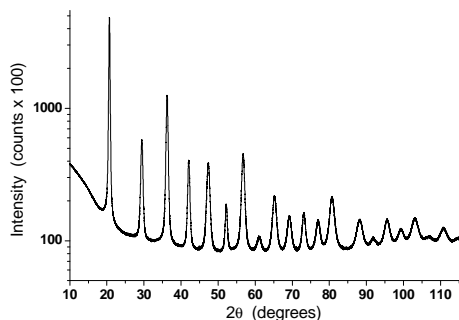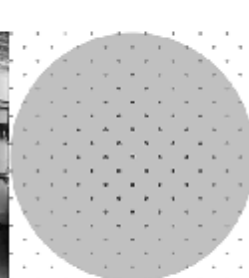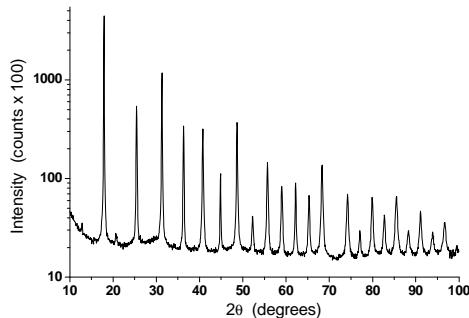
P. Scardi – Diffraction from nanocrystalline materials

SYNCHROTRON RADIATION X-RAY DIFFRACTION

- increase energy **à** extend Ewald sphere!
- increase energy **à** high $Q(=4\pi\sin\theta/\lambda)$ for PDF analysis
- statistics /short time /kinetics / in situ / in operando
- control absorption and instrumental effects
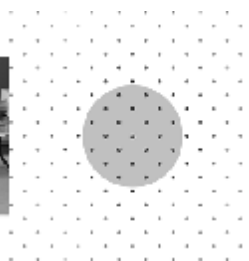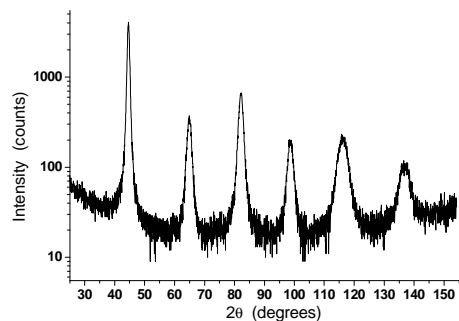
Powder diffraction data from a ball milled Fe1.5%Mo powder collected (a) on a traditional laboratory instrument (Rigaku PMG-VH, Bragg-Brentano geometry) with CuKα radiation (λ=0.1540598 nm) and SR (Debye-Scherrer geometry): (b) ID31 (now ID22) at ESRF, Grenoble (F) (λ=0.0632 nm), and (c) MS-X04SA at PSI, Villigen (CH) (λ=0.072929 nm). On the right: schematic of reciprocal space with extension of the limiting sphere (radius 2/λ).
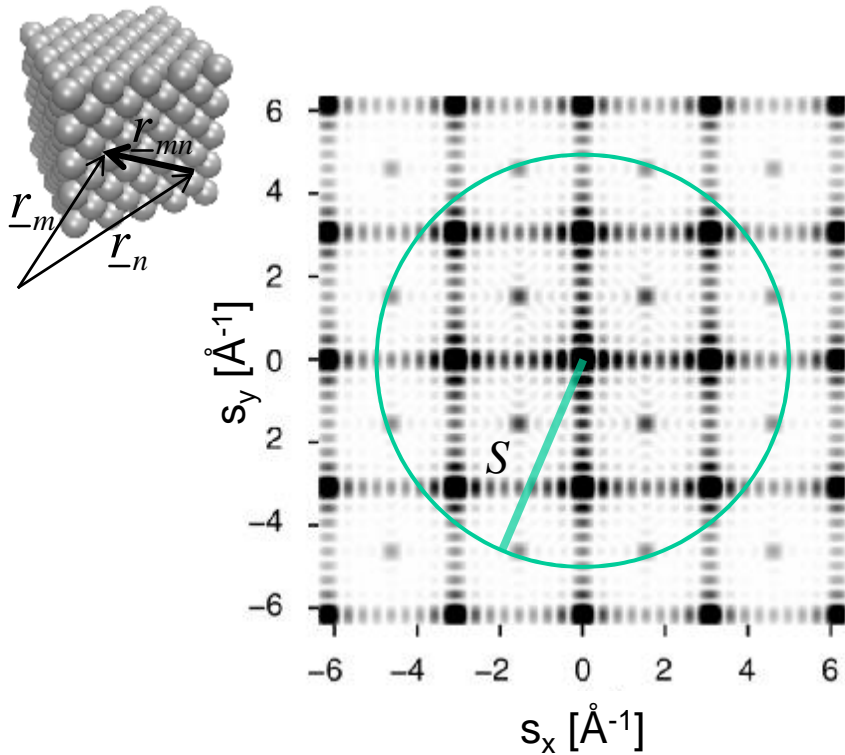
P. Scardi & L. Gelisio, "Diffraction from nanocrystalline materials", in Synshrotron radiation, ed. S. Mobilio et al., Springer 2015. Chap. XVIII,.
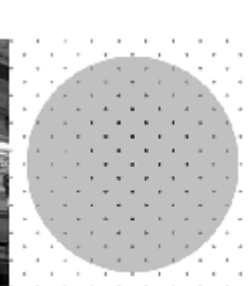
Powder diffraction and synchrotron radiation: visit the MCX beamline at ELETTRA (J.R. Plaisier)

orientational
(or powder)
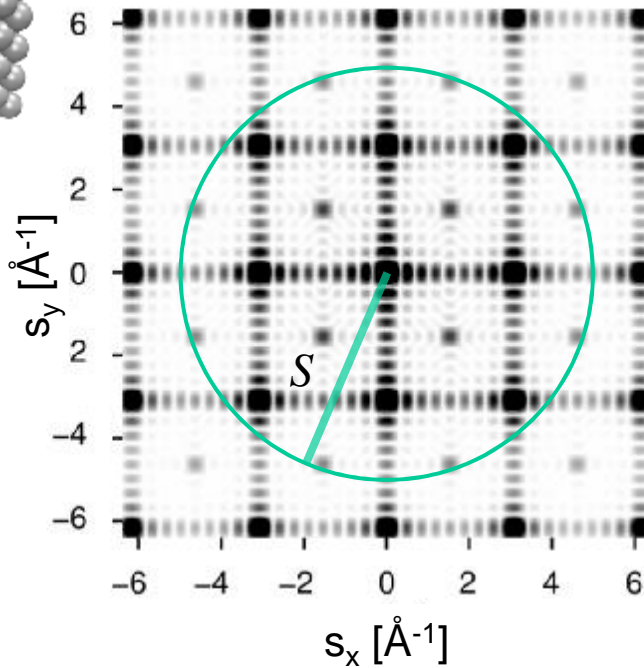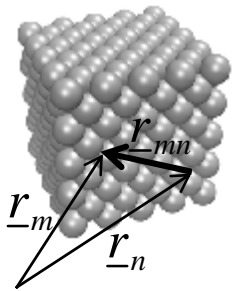average

$$s = Q/2\pi = 2\sin\theta\,/\lambda$$

$$I_{PD}(s) \propto \frac{\int I_{sc}(\underline{s})d\Omega}{4p\,s^2}$$

$$d\Omega = s^2 \sin J\,dJ\,df$$

$$I_{sc}(\underline{s}) \propto \sum_m f_m e^{2pi(\underline{s}\cdot\underline{r}_m)} \sum_n f_n^* e^{-2pi(\underline{s}\cdot\underline{r}_n)} = \sum_m \sum_n f_m f_n^* e^{2pi(\underline{s}\cdot\underline{r}_{mn})}$$
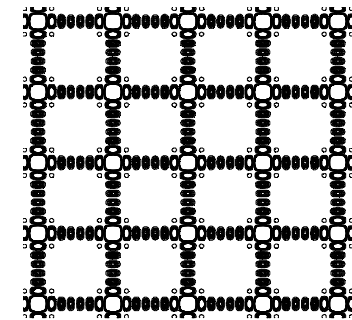
DIFFRACTION FROM NANOCRYSTALLINE *POWDER*

(1) sum, then average

or

(2) average, then sum

Debye scattering equation, "direct space"
Total scattering approach

$$I_{PD}(s) \propto \frac{\int \sum_m \sum_n f_m f_n^* e^{2pi(\underline{s} \cdot \underline{r}_{mn})} d\Omega}{4p\, s^2}$$

$$s = Q/2\pi = 2\sin\theta\, /\lambda$$

$$d\Omega = s^2 \sin J\, dJ\, df$$

$$I_{sc}(\underline{s}) \propto \sum_m f_m e^{2pi(\underline{s} \cdot \underline{r}_m)} \sum_n f_n^* e^{-2pi(\underline{s} \cdot \underline{r}_n)} = \sum_m \sum_n f_m f_n^* e^{2pi(\underline{s} \cdot \underline{r}_{mn})}$$

DIFFRACTION FROM NANOCRYSTALLINE *POWDER*
Traditional "reciprocal space" approach (sum, then average)

1. Factorize the contribution of a unit cell
   ($|F|^2 - F$, structure factor)

$$D = Na \quad\updownarrow\quad a$$
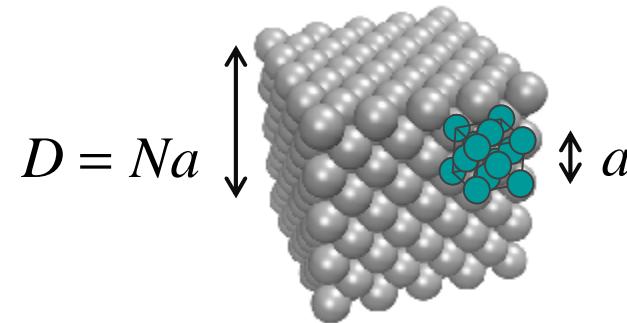
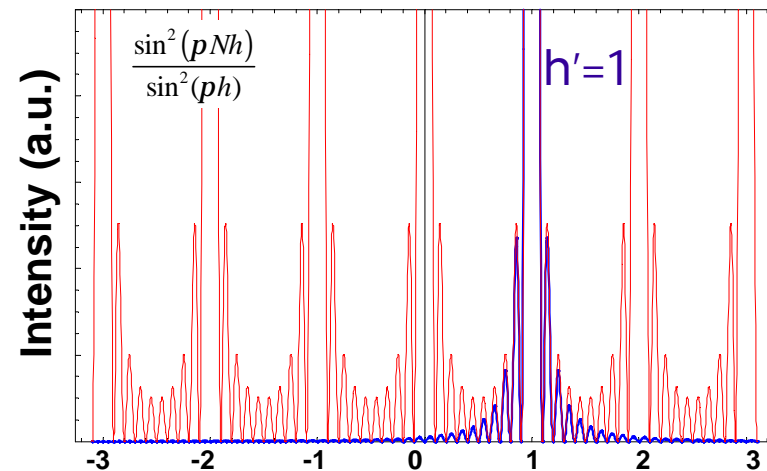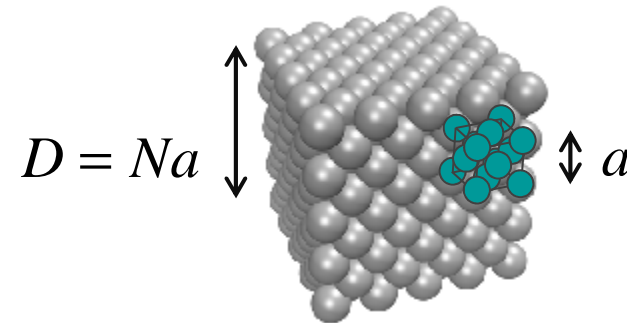2. Build the diffraction signal as interference between unit cells

$$I_{sc} \propto |F|^2 \sum_{h'=-\infty}^{\infty} \sum_{k'=-\infty}^{\infty} \sum_{l'=-\infty}^{\infty} \frac{\sin^2(pNh)}{p^2(h-h')^2} \frac{\sin^2(pNk)}{p^2(k-k')^2} \frac{\sin^2(pNl)}{p^2(l-l')^2}$$

Integral Breadth (*b*) of a (h00) peak:

$$b = \frac{\displaystyle\int_{-\infty}^{\infty} \frac{\sin^2(pNh)}{p^2(h-1)^2}\,dh}{I(h=1)} = \frac{N}{N^2} = \frac{1}{N} \propto \frac{1}{D}$$

Scherrer equation

$$\frac{\sin^2(pNh)}{\sin^2(ph)} \qquad h'=1$$

Intensity (a.u.)

h

-3   -2   -1   0   1   2   3

DIFFRACTION FROM NANOCRYSTALLINE *POWDER*
Traditional "reciprocal space" approach (sum, then average)

1. Factorize the contribution of a unit cell
   ($|F|^2 - F$, structure factor)

$$D = Na \qquad \updownarrow a$$

2. Build the diffraction signal as interference between unit cells

$$I_{sc} \propto |F|^2 \sum_{h'=-\infty}^{\infty} \sum_{k'=-\infty}^{\infty} \sum_{l'=-\infty}^{\infty} \frac{\sin^2(pNh)}{p^2(h-h')^2} \frac{\sin^2(pNk)}{p^2(k-k')^2} \frac{\sin^2(pNl)}{p^2(l-l')^2}$$
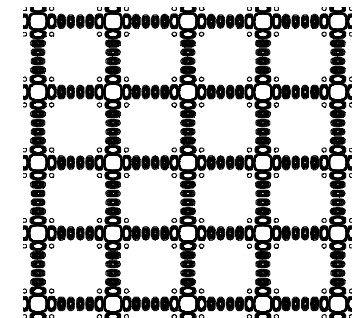
3. Integrate over the powder diffraction sphere (orientational average)

$$I_{PD}(s) \propto \frac{\int I_{sc}(\underline{s})\,d\Omega}{4ps^2} \implies$$

s_y [Å⁻¹]

s_x [Å⁻¹]
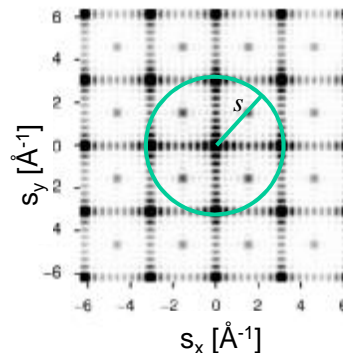
$$\boxed{I(q) \propto |F|^2\, \Phi(q, D)}$$

$\underbrace{}$

line profile
function

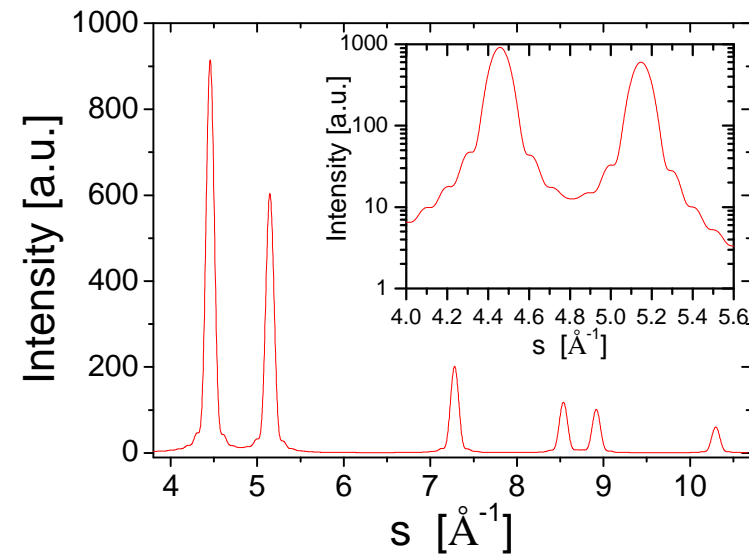# DIFFRACTION FROM NANOCRYSTALLINE *POWDER*

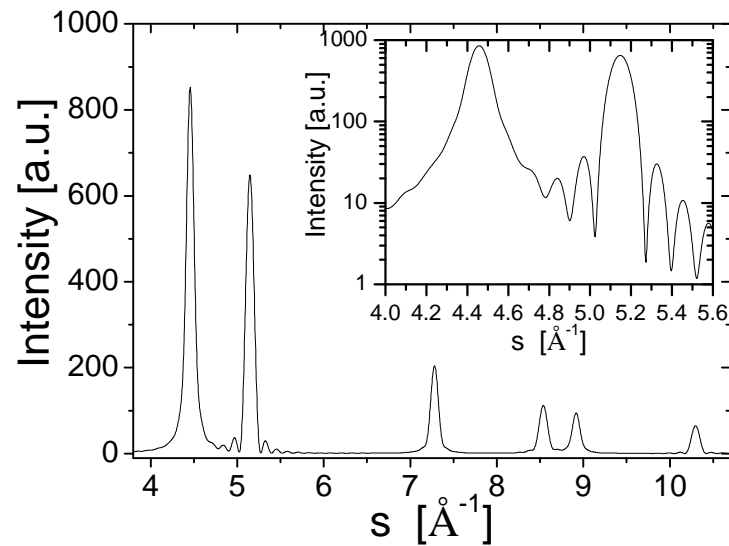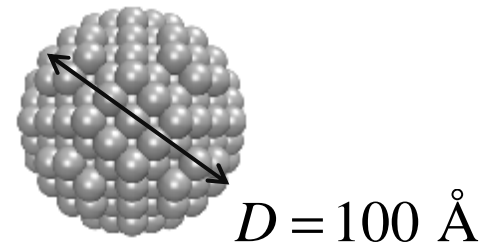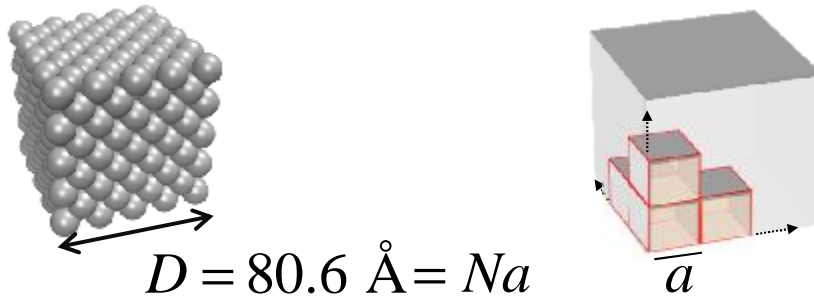## small cubic / spherical fcc domains
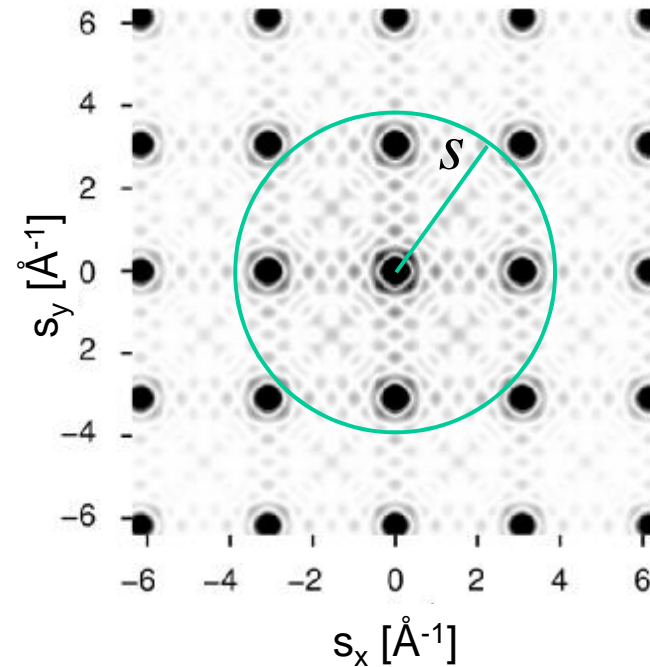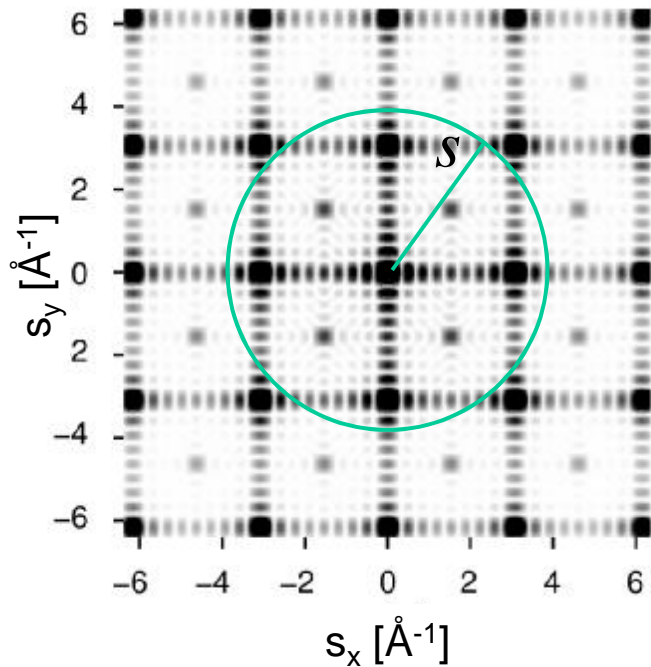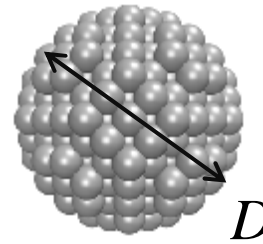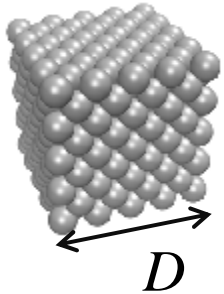
$$I_{PD}(s) \propto |F|^2 \Phi_{cube}(s,D)$$

$$I_{PD}(s) \propto |F|^2 \Phi_{sphere}(s,D)$$

DIFFRACTION FROM NANOCRYSTALLINE *POWDER*

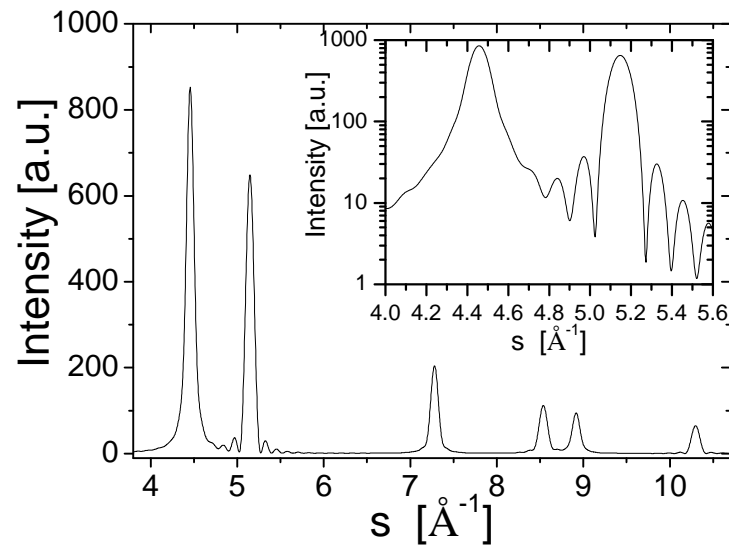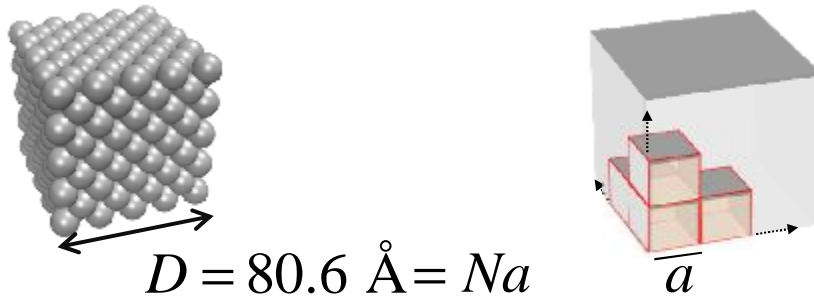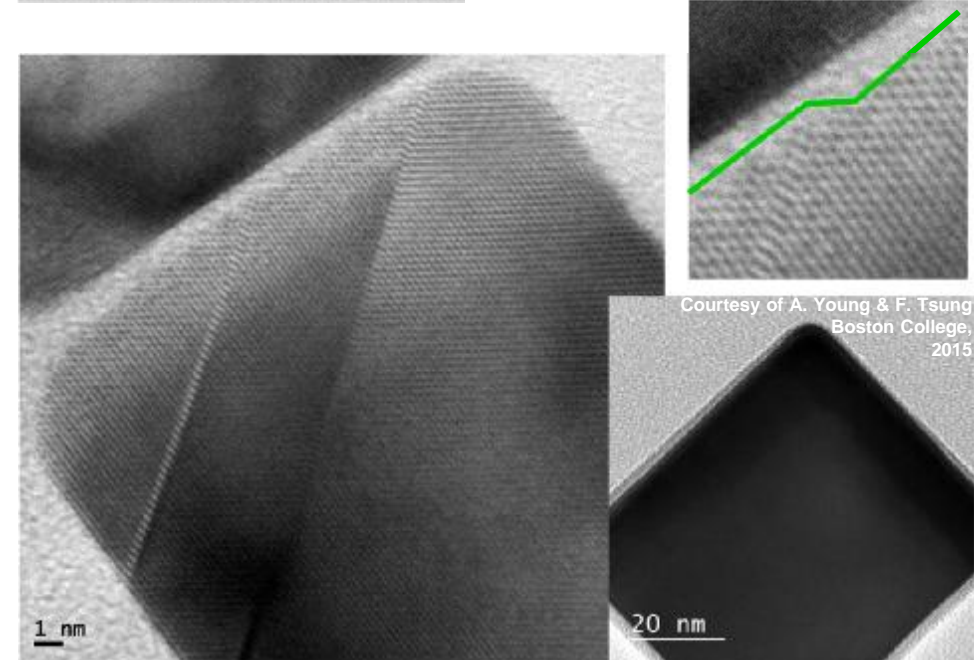## small cubic   /   spherical fcc domains

$$D = 80.6 \text{ Å} = Na$$

$$\overline{a}$$

$$D = 100 \text{ Å}$$

$$I_{PD}(s) \propto |F|^2 \Phi_{cube}(s, D)$$

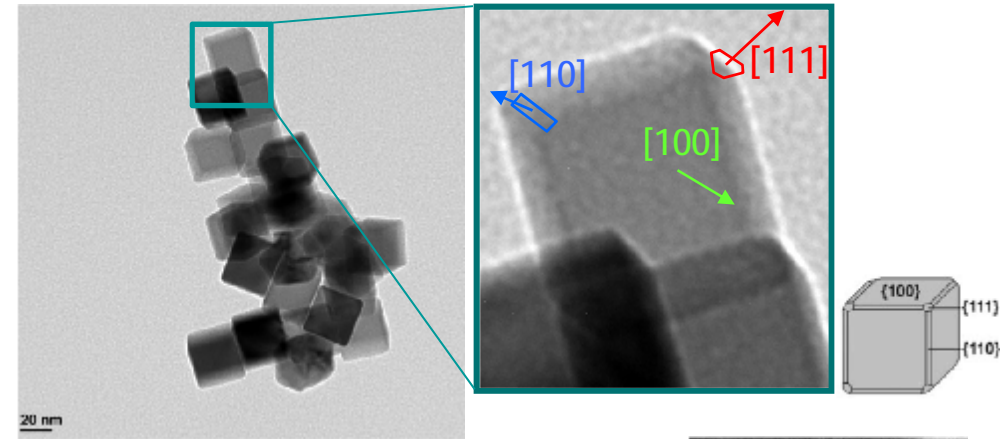$$I_{PD}(s) \propto |F|^2 \Phi_{sphere}(s, D)$$

IDEAL vs REAL NANOCRYSTALS
Microstructure: any deviation from perfect crystalline order

$$D = 80.6 \ \text{Å} = Na$$

$\overline{a}$

$$I_{PD}(s) \propto |F|^2 \Phi_{cube}(s,D)$$

Pd nanocrystals

Solla-Gullon et al., J. Appl. Cryst. 48 (2015) 1534

[110] [111] [100]
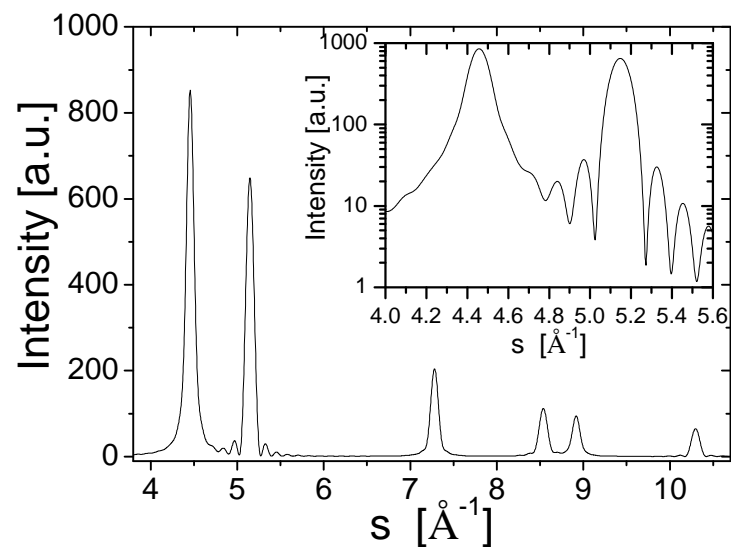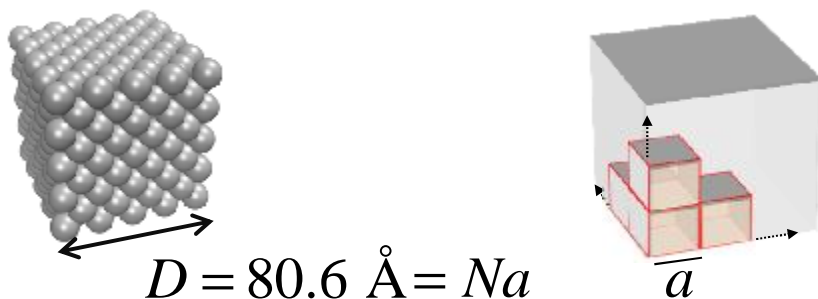
20 nm

{100} {111} {110}

Courtesy of A. Young & F. Tsung
Boston College,
2015

1 nm   20 nm

P. Scardi – Diffraction from nanocrystalline materials

IDEAL vs REAL NANOCRYSTALS
Microstructure: any deviation from perfect crystalline order

$$D = 80.6 \text{ Å} = Na$$

$$\overline{a}$$

Pd nanocrystals

Solla-Gullon et al., J. Appl. Cryst. 48 (2015). In press.

[110]   [111]
[100]

{100} {111} {110}

20 nm

-0.50   0.05(Å)
0.45   0.00(Å)
0.30   0.00(Å)
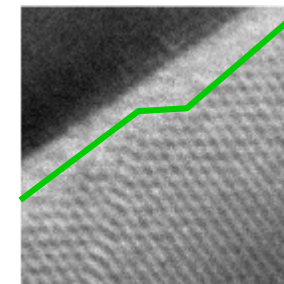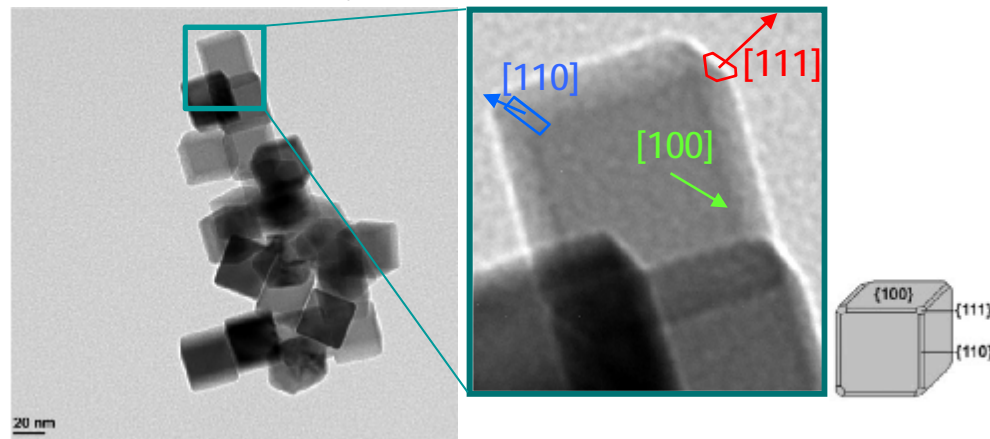
10 nm

Courtesy of A. Young & F. Tsung
Boston College,
2015

20 nm
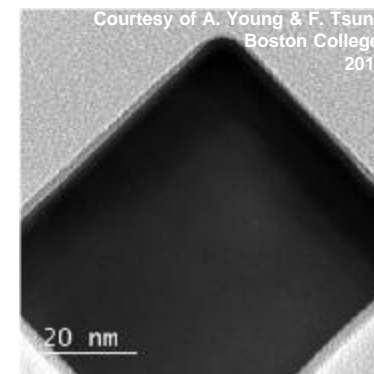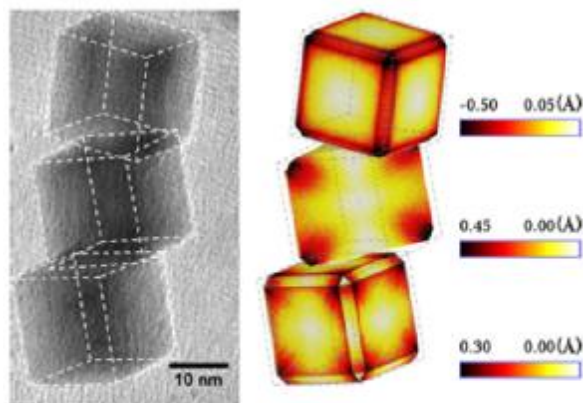
FIG. 6. (Color online) TEM picture of Pd nanocubes (left, dash is drawn just to drive the eye) with corresponding atomic displacement maps (right) for: normal component on the surface (top), norm of the component projected on the (110) cross section (middle), and on the surface of the nanocrystal (bottom).
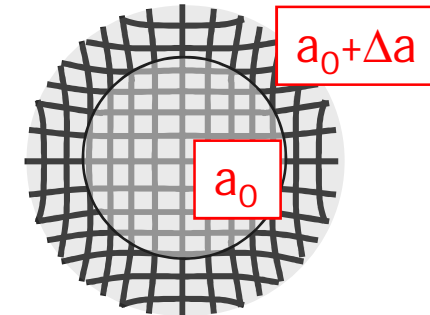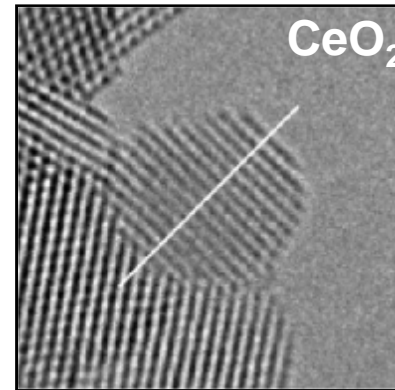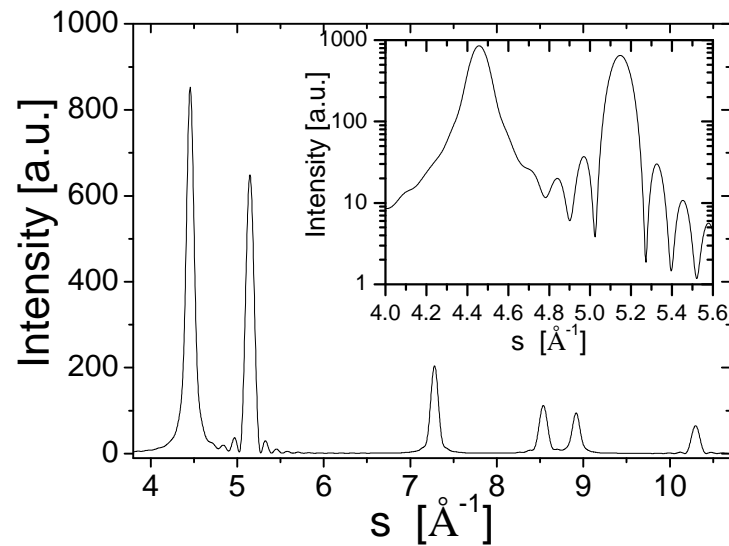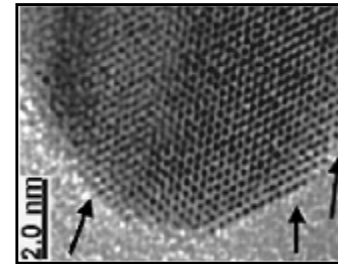
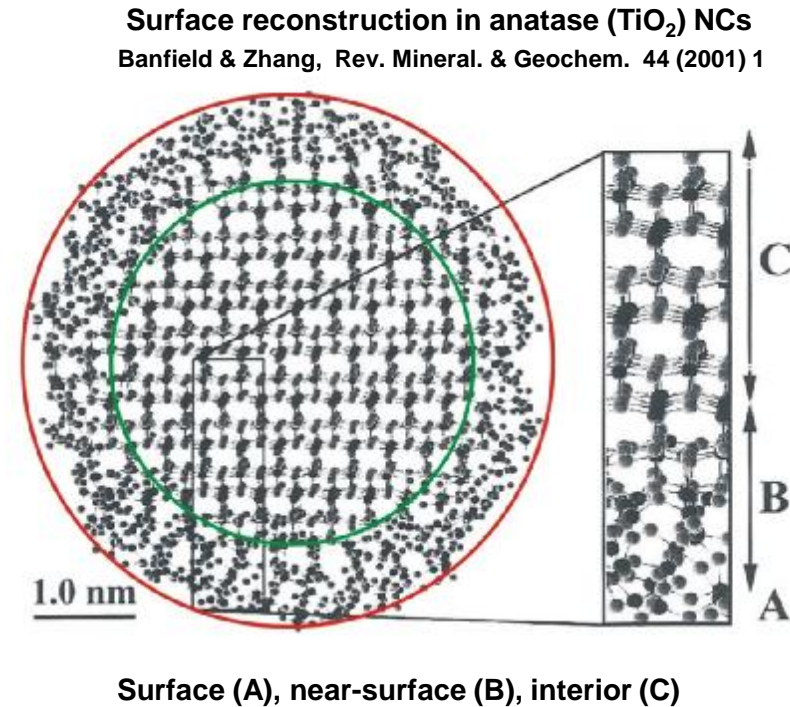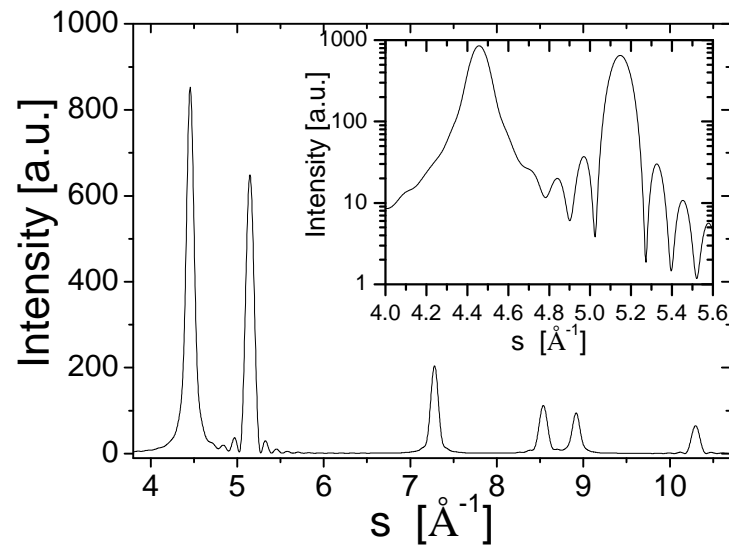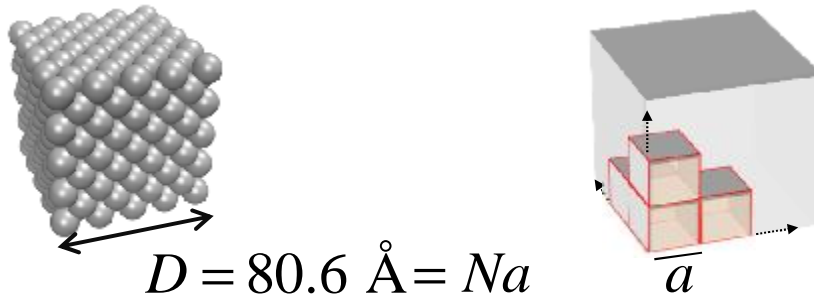**Scardi et al., Phys.Rev. B 91 (2015) 155414**

$$I_{PD}(s) \propto |F|^2 \Phi_{cube}(s, D)$$

IDEAL vs REAL NANOCRYSTALS
Microstructure: any deviation from perfect crystalline order

$$D = 80.6 \ \text{Å} = Na$$

$$\overline{a}$$
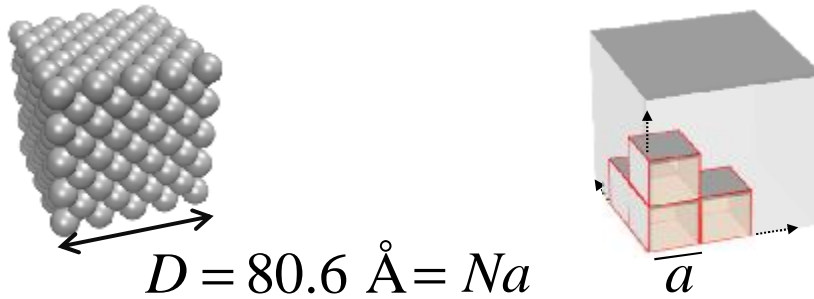
**Surface relaxation in nanocrystals**

CeO$_2$

a$_0$+Δa

a$_0$

$$I_{PD}(s) \propto |F|^2 \ \Phi_{cube}(s,D)$$

IDEAL vs REAL NANOCRYSTALS
Microstructure: any deviation from perfect crystalline order

$$D = 80.6 \text{ Å} = Na$$

$\overline{a}$

Surface reconstruction in anatase (TiO$_2$) NCs
Banfield & Zhang, Rev. Mineral. & Geochem. 44 (2001) 1

1.0 nm

Surface (A), near-surface (B), interior (C)

$$I_{PD}(s) \propto |F|^2 \Phi_{cube}(s, D)$$

IDEAL vs REAL NANOCRYSTALS
Microstructure: any deviation from perfect crystalline order

$$D = 80.6 \text{ Å} = Na$$

$$\overline{a}$$
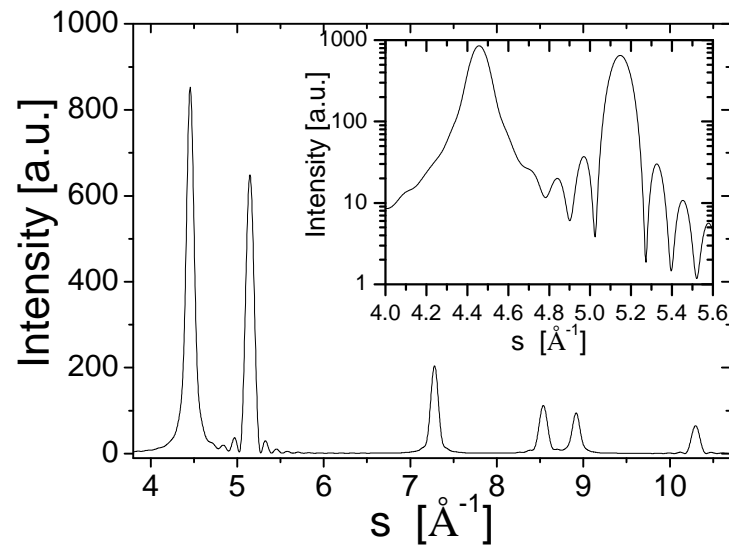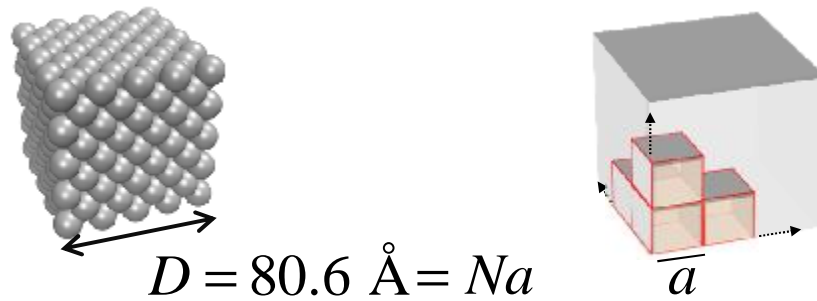
Ball-milled Fe-Mo alloy

Rebuffi et al., Nat. Sci. Reports 6 20712 (2016)

$$I_{PD}(s) \propto |F|^2 \Phi_{cube}(s, D)$$
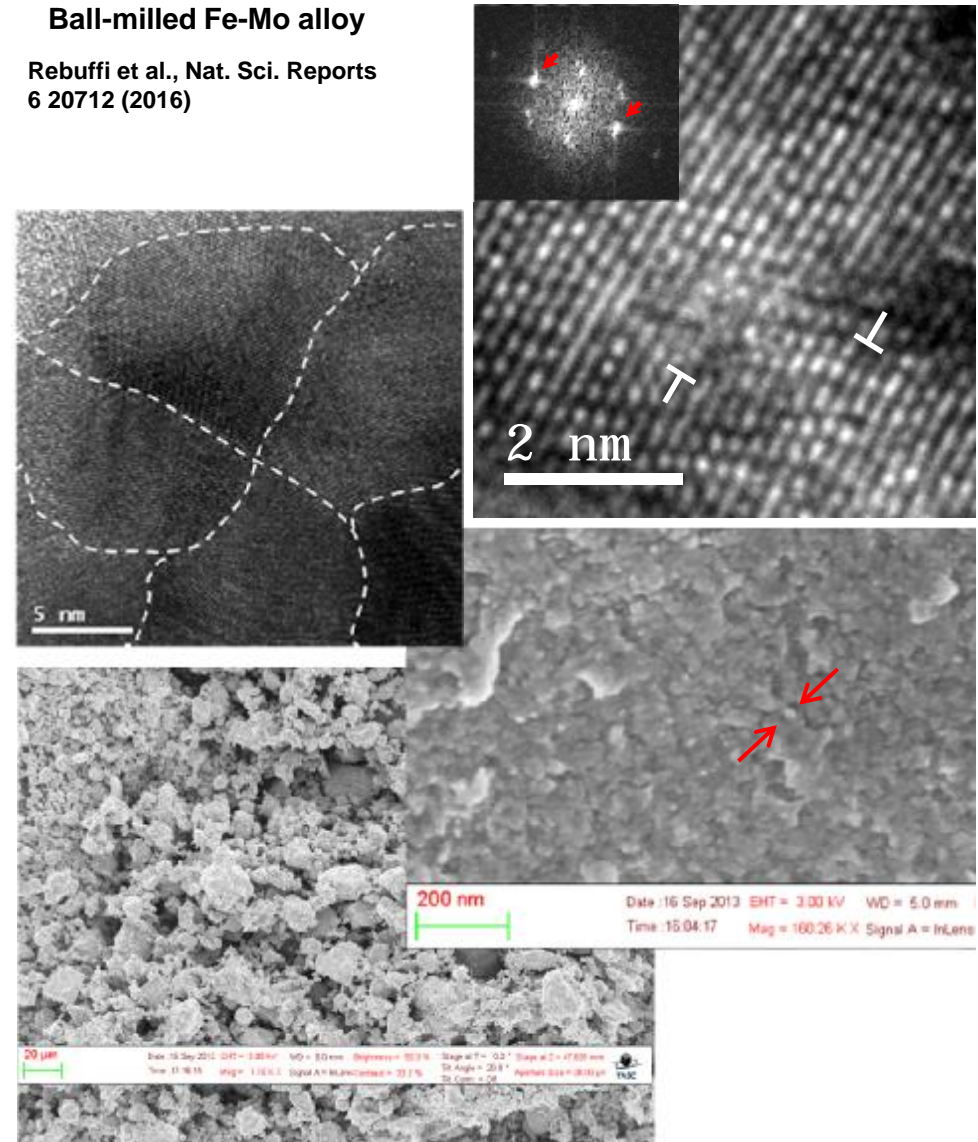
DIFFRACTION PATTERN FROM A POLYCRYSTALLINE

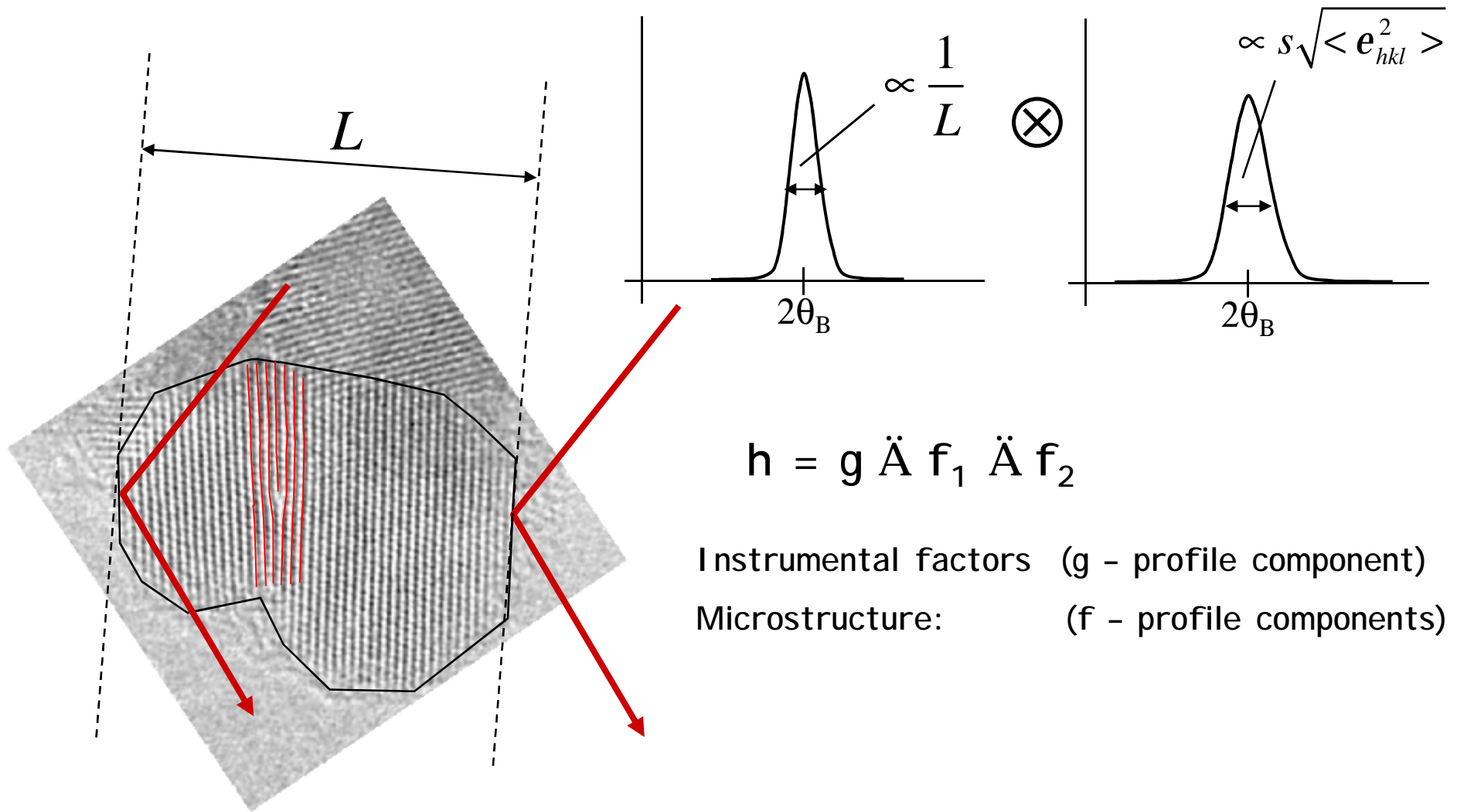Experimental peak profiles (h) can be represented as a convolution :

$$h = g \otimes f_1 \otimes f_2 \otimes f_3 \otimes \ldots$$

Ø Instrumental factors: (g – profile component)

Ø Microstructure: (f – profile components)

line broadening from instrument, domain size/shape and dislocations

$$\propto \frac{1}{L} \quad \otimes \quad \propto s\sqrt{<e_{hkl}^2>}$$

$2\theta_B$ $2\theta_B$

$$\mathsf{h = g\ Ä\ f_1\ Ä\ f_2}$$

Instrumental factors   (g – profile component)

Microstructure: (f – profile components)

DOMAIN SIZE AND MICROSTRAIN BROADENING

## Dislocation line broadening is markedly anisotropic, i.e., *hkl* dependent

$$\propto s\sqrt{<e_{hkl}^2>}$$

$2\theta_B$

$\underline{d}_{hkl}^*$

$\underline{d}_{hkl}^*$

dislocation visibility depends on the viewing direction

DOMAIN SIZE AND MICROSTRAIN BROADENING

Dislocation line broadening is markedly anisotropic, i.e., *hkl* dependent

$$\propto s\sqrt{<e_{hkl}^2>}$$

$\underline{d}^*_{hkl}$

$\underline{d}^*_{hkl}$

$2\theta_B$

'invisible'
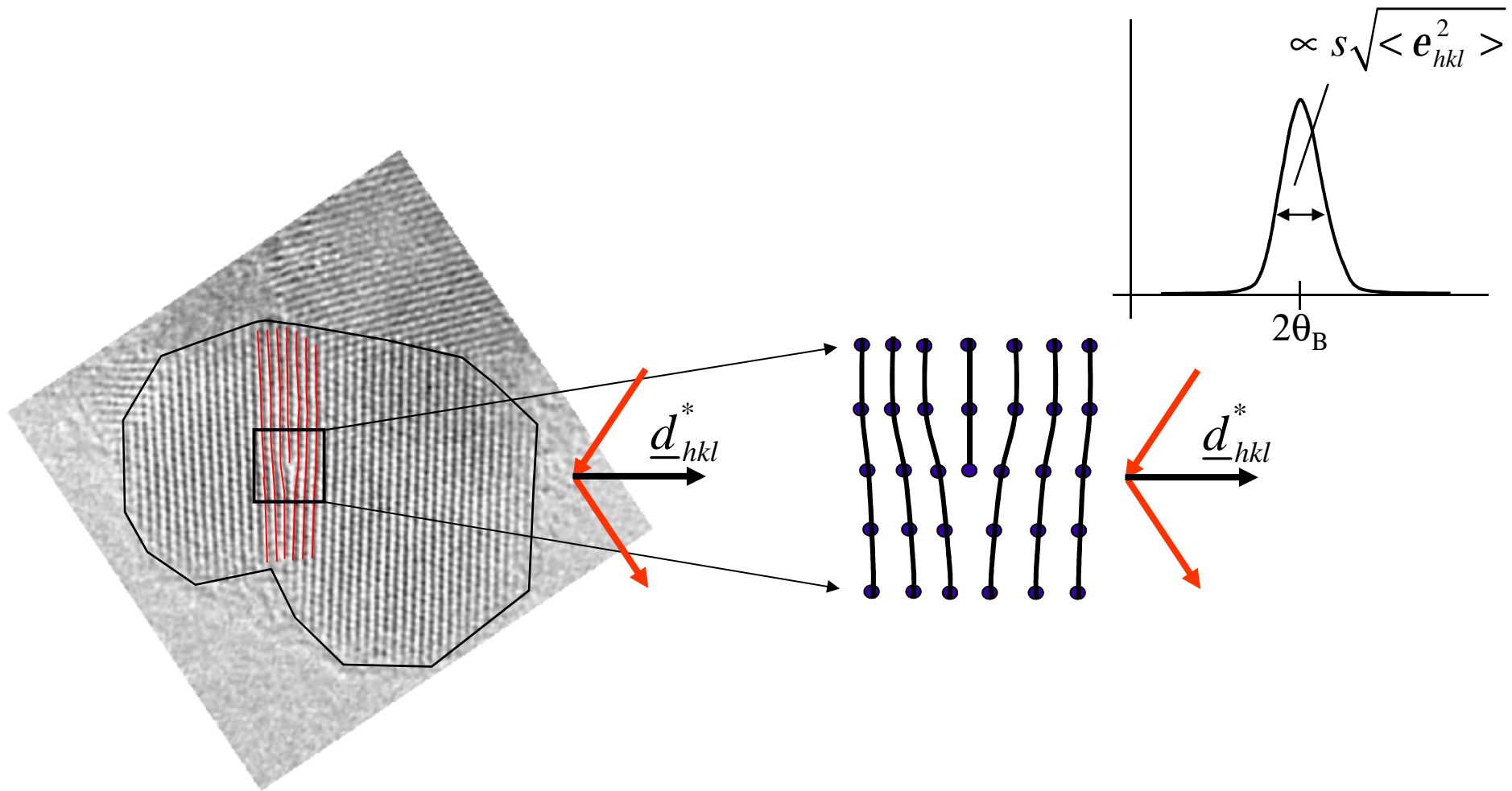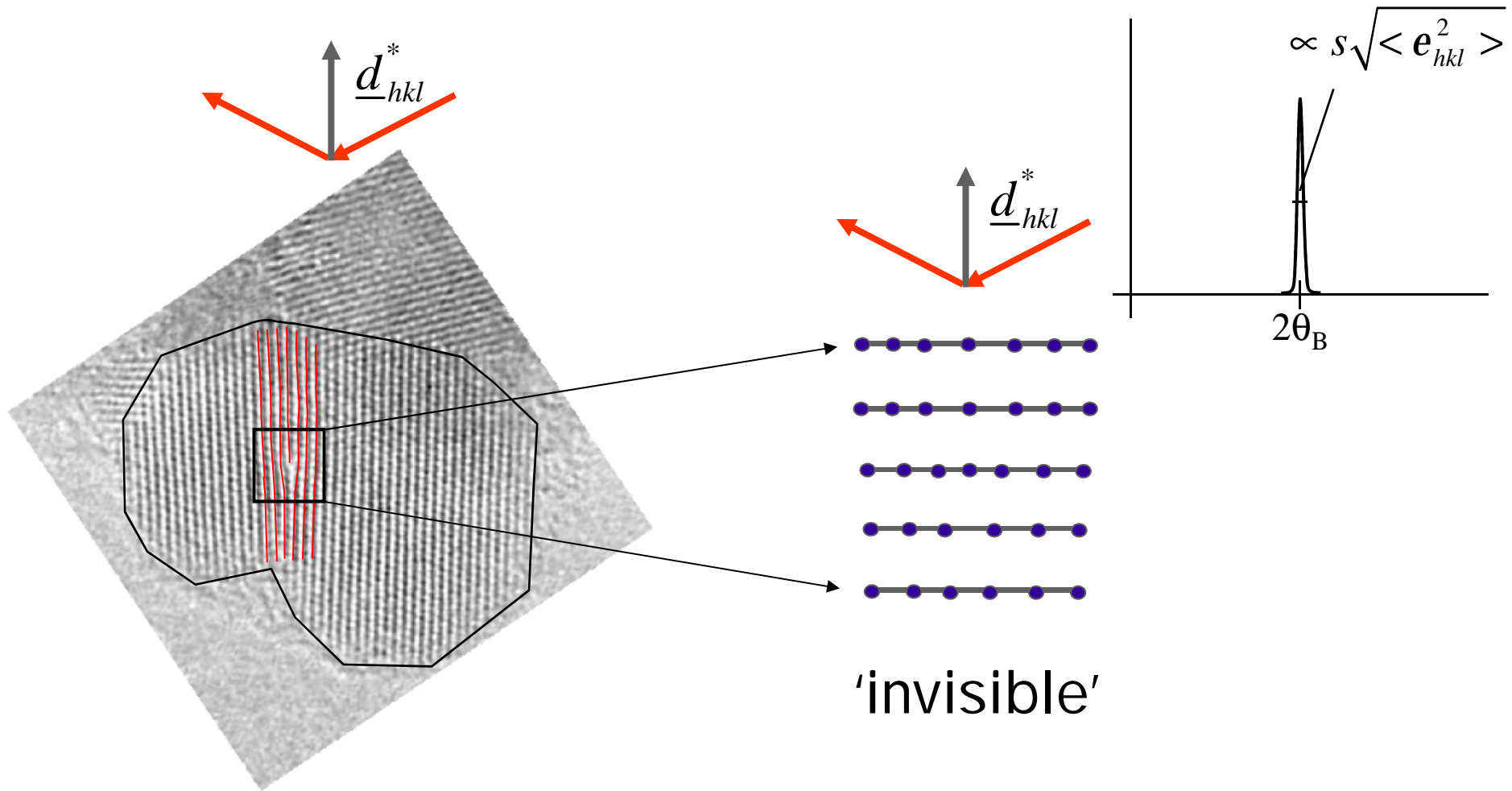
dislocation visibility depends on the viewing direction

DOMAIN SIZE AND MICROSTRAIN BROADENING

Combined line broadening effect from domain size and dislocations

$$\propto \frac{1}{L} \qquad \otimes \qquad \propto s\sqrt{<e_{hkl}^2>}$$

$2\theta_B \qquad 2\theta_B$

L

$$h = g \; Ä \; f_1 \; Ä \; f_2 \; Ä \; f_3 \; Ä \; f_4 \; Ä \; ...$$

Instrumental factors   (g – profile component)

Microstructure: (f – profile components)
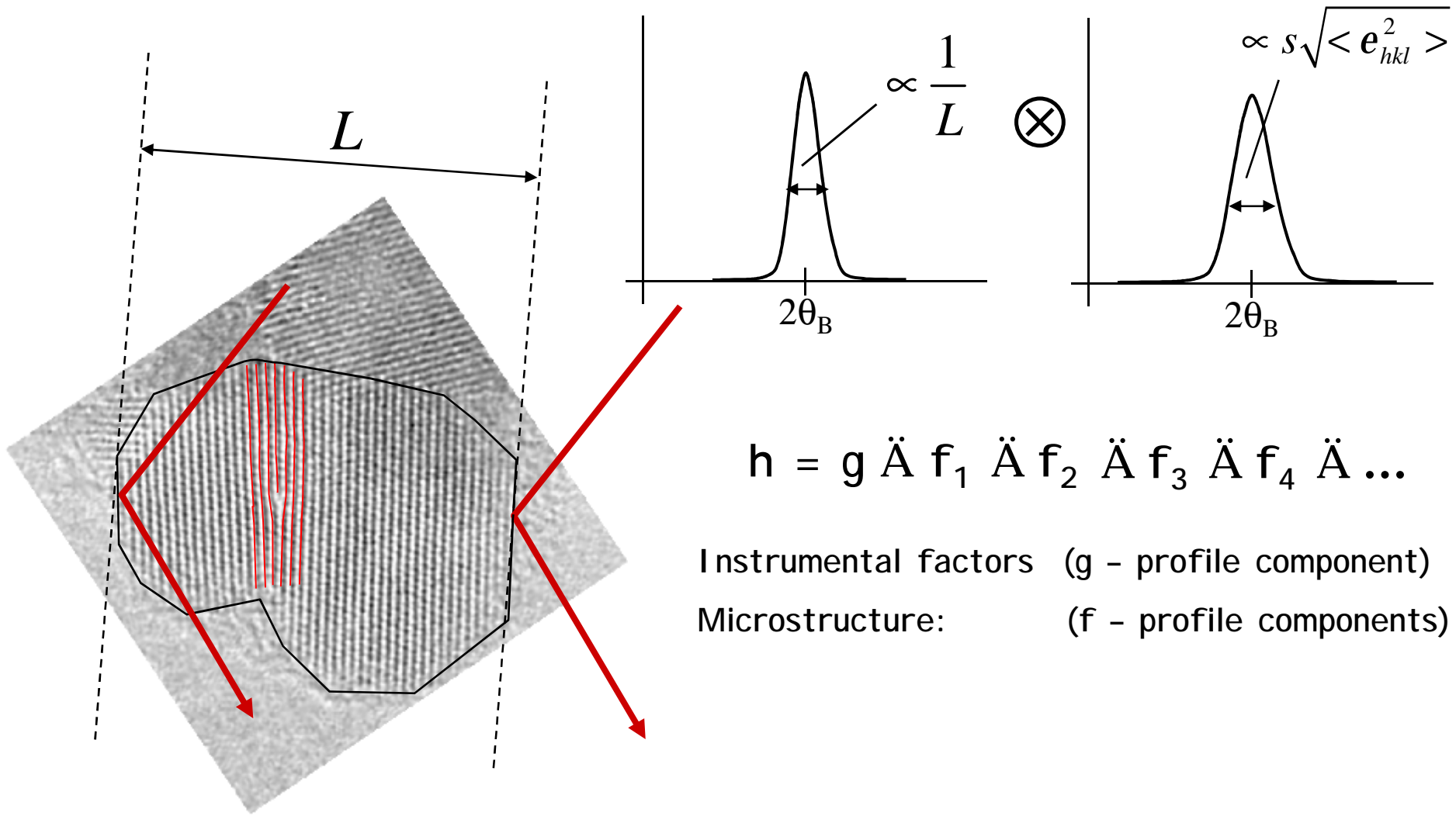
DIFFRACTION PATTERN FROM A POLYCRYSTALLINE

Most common line broadening sources
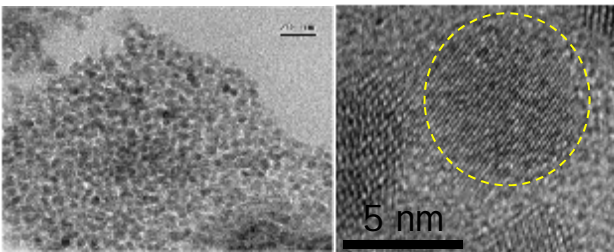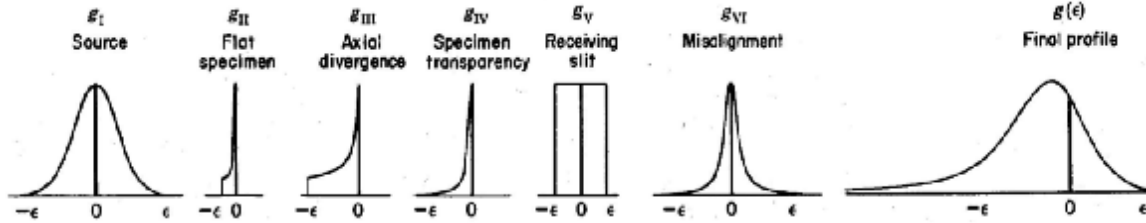
Grain shape and size distribution
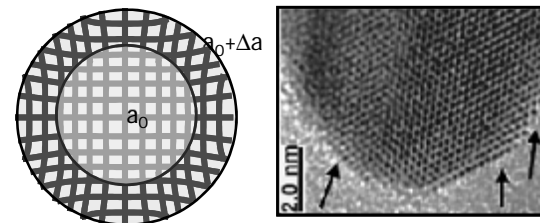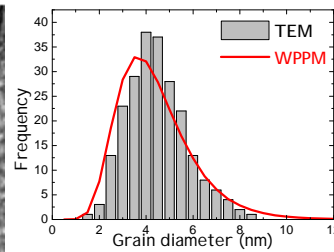
Grain surface relaxation
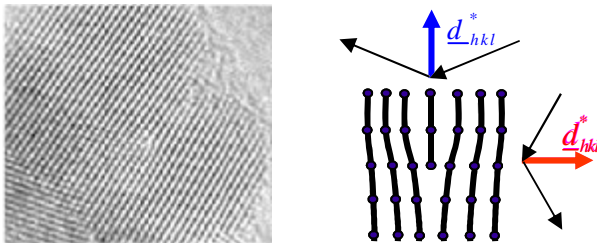
dislocations, disclinations
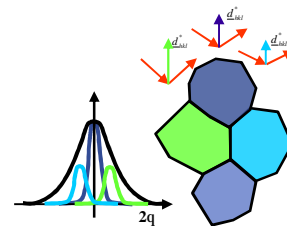
stoichiometry fluctuation
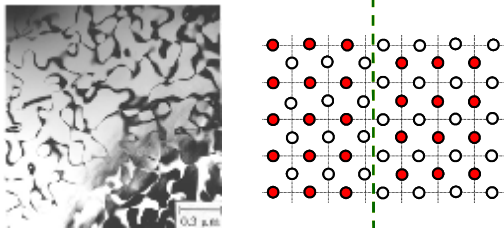
Anti-phase boundaries
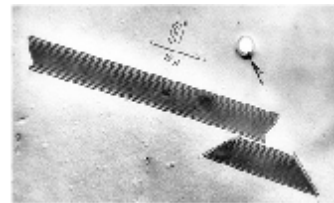
Stacking faults

g

$f_1 \otimes f_2 \otimes f_3 \otimes \ldots$

Diffraction profile as a convolution of (independent) effects:

$$I(s) = I^{IP}(s) \otimes I^{S}(s) \otimes I^{D}(s) \otimes I^{F}(s) \otimes I^{APB}(s) \otimes \ldots$$

the Fourier Transform of I(s) is the product of the FTs of the single profile components

$$I(s) \propto \cdot \int_{-\infty}^{\infty} C(L) e^{2\pi i L \cdot s_{hkl}} \, dL$$

$$C = \prod_i A_i = T_{pV}^{IP} \cdot A_{\{hkl\}}^{S} \cdot A_{\{hkl\}}^{D} \cdot (A_{hkl}^{F} + i B_{hkl}^{F}) \cdot A_{\{hkl\}}^{APB} \cdot \ldots$$

instr. profile   domain size/shape   microstrain / lattice defects/…

P. Scardi, Chap. 13 in Powder Diffraction: Theory and Practice, R.E. Dinnebier & S.J.L. Billinge, eds. RSC, Cambridge, 2008

WPPM : HOW DOES IT WORK ??

$$T_{pV}^{IP}(L) = (1-k) \cdot \exp\left(-p^2 \cdot s_s^2 L^2 / \ln 2\right) + k \exp(-2p \cdot s_s L)$$ <u>Instrumental profile</u>

<u>Domain size effect: *m, s*</u>

$$A^S(L) = \sum_{n=0}^{3} H_n^c \cdot Erfc\left[\frac{\ln(L \cdot K^c) - m - (3-n)s^2}{s\sqrt{2}}\right] \frac{M_{l,3-n}}{2M_{l,3}} \cdot L^n$$
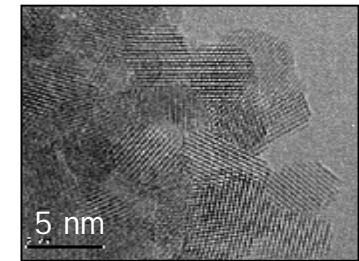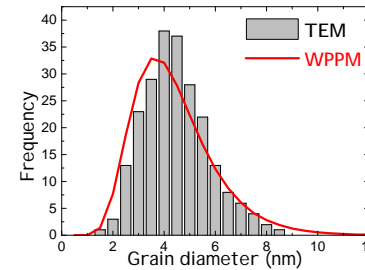
<u>Dislocation (strain) effect: *r, Re, ($\overline{C}_{hkl}$)*</u>

$$A_{\{hkl\}}^D(L) = \exp\left[-\frac{1}{2}p|b|^2 \overline{C}_{hkl} \, r d_{\{hkl\}}^{*2} \cdot L^2 f^*(L/R_e)\right]$$

$$\overline{C}_{hkl} = A + B \cdot \frac{h^2 k^2 + k^2 l^2 + l^2 h^2}{(h^2+k^2+l^2)^2} = A + B \cdot H$$
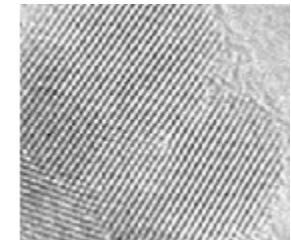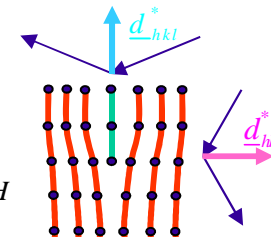
<u>Faulting: *a* (def.), *b* (twin)</u>

$$A_{hkl}^F(L) = (1-3a-2b+3a^2)^{\left|\frac{1}{2}Ld_{\{hkl\}}^* \cdot \frac{L_o}{h_o^2} s_{L_o}\right|}$$

$$B_{hkl}^F(L) = -s_{L_o} \cdot \frac{L}{|L|} \cdot \frac{L_o}{|L_o|} \cdot b \Big/ (3-6b-12a-b^2+12a^2)^{1/2}$$
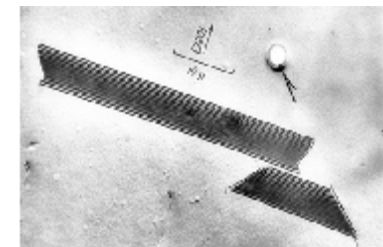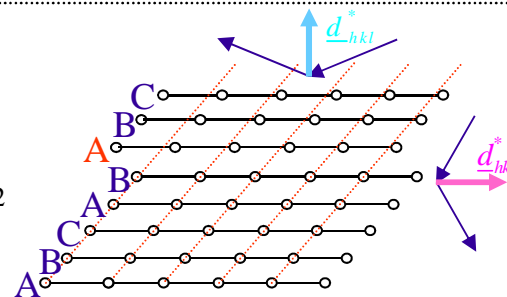
<u>Anti-Phase Domains: *g*</u>

$$A_{\{hkl\}}^{APB}(L) = \exp\left[-\frac{-2g(|h|+|k|) \cdot L}{d_{hkl}(h^2+k^2+l^2)}\right]$$
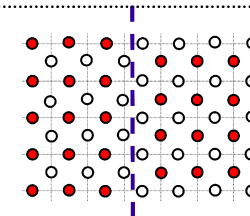
WHOLE POWDER PATTERN MODELLING - WPPM

based on physical models of the microstructure

$$I(s) \propto \cdot \int_{-\infty}^{\infty} C(L) e^{2\pi iL \cdot s_{hkl}} \, dL$$

$$C = \prod_i A_i = T_{pV}^{IP} \cdot A_{\{hkl\}}^{S} \cdot A_{\{hkl\}}^{D} \cdot (A_{hkl}^{F} + iB_{hkl}^{F}) \cdot A_{\{hkl\}}^{APB} \cdot \ldots$$

instr.   domain   microstrain / lattice defects/...
profile   size/shape

Direct modelling of diffraction profiles in terms of relatively few microstructural parameters: m, s - r, R_e - a, b - g ...
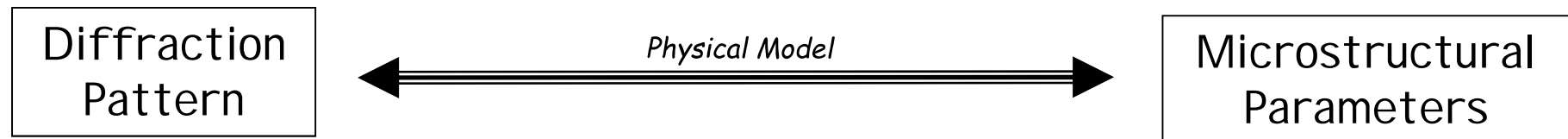
Diffraction Pattern	Physical Model	Microstructural Parameters

P. Scardi, Chap. 13 in Powder Diffraction: Theory and Practice, R.E. Dinnebier & S.J.L. Billinge, eds. RSC, Cambridge, 2008

MCX - ELETTRA
λ=0.082666 nm
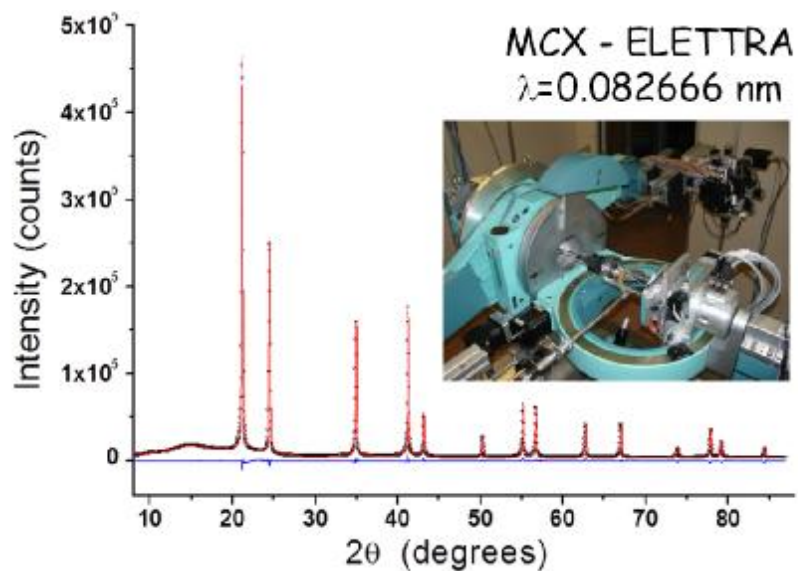
"identical" Pd nanoparticles

Ball milled Fe-1.5%Mo

ESRF – ID31
λ=0.0632 nm
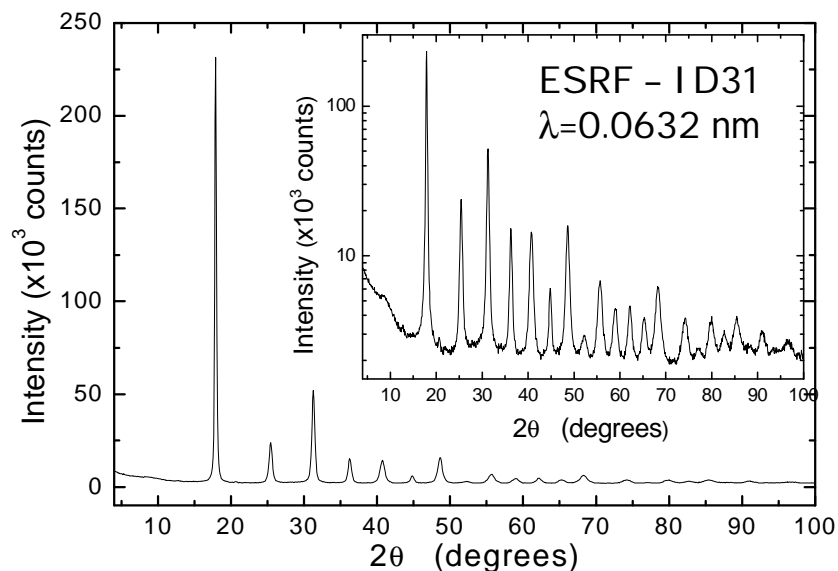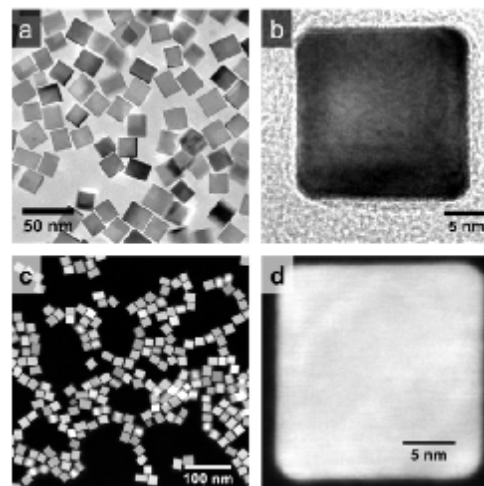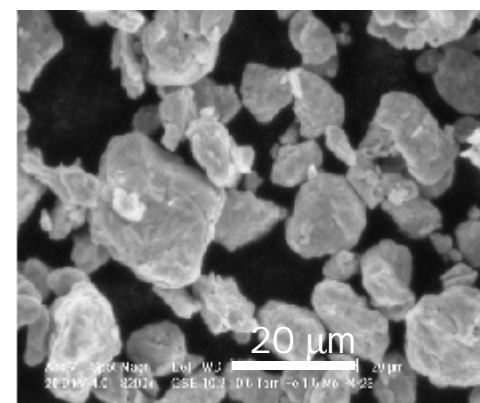
NANOCRYSTALLINE Fe-1.5%Mo POWDER

Planetary ball milling - production of nanocrystalline Fe-1.5%Mo
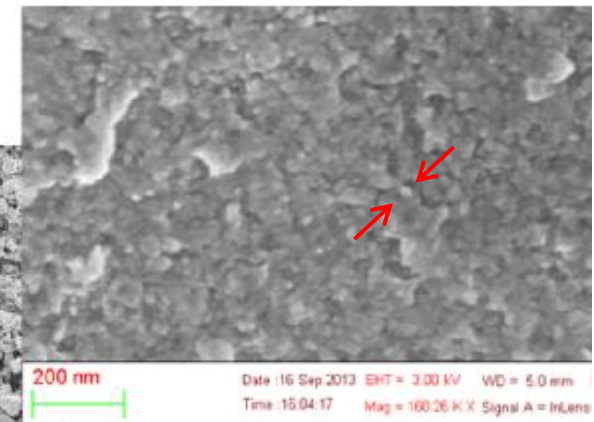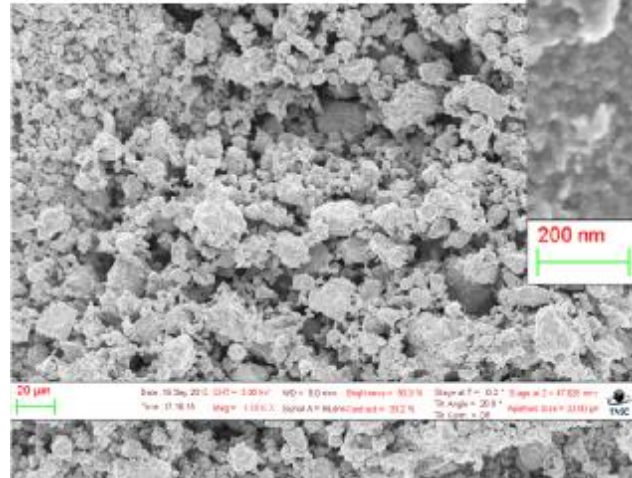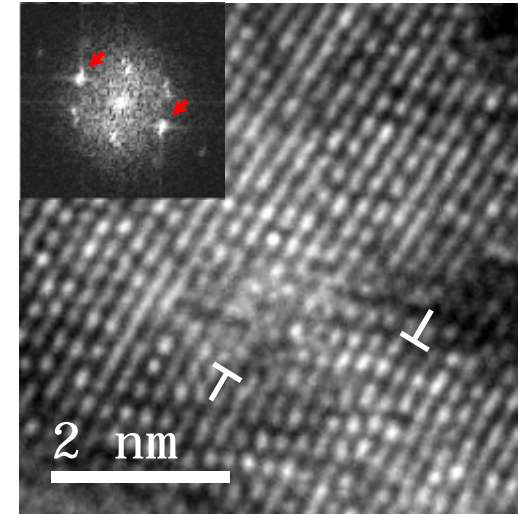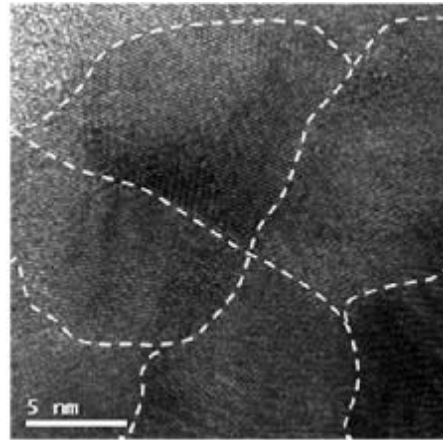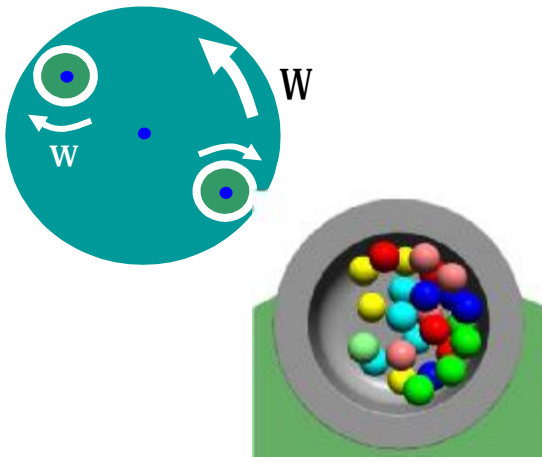
2 nm

5 nm

200 nm

20 µm
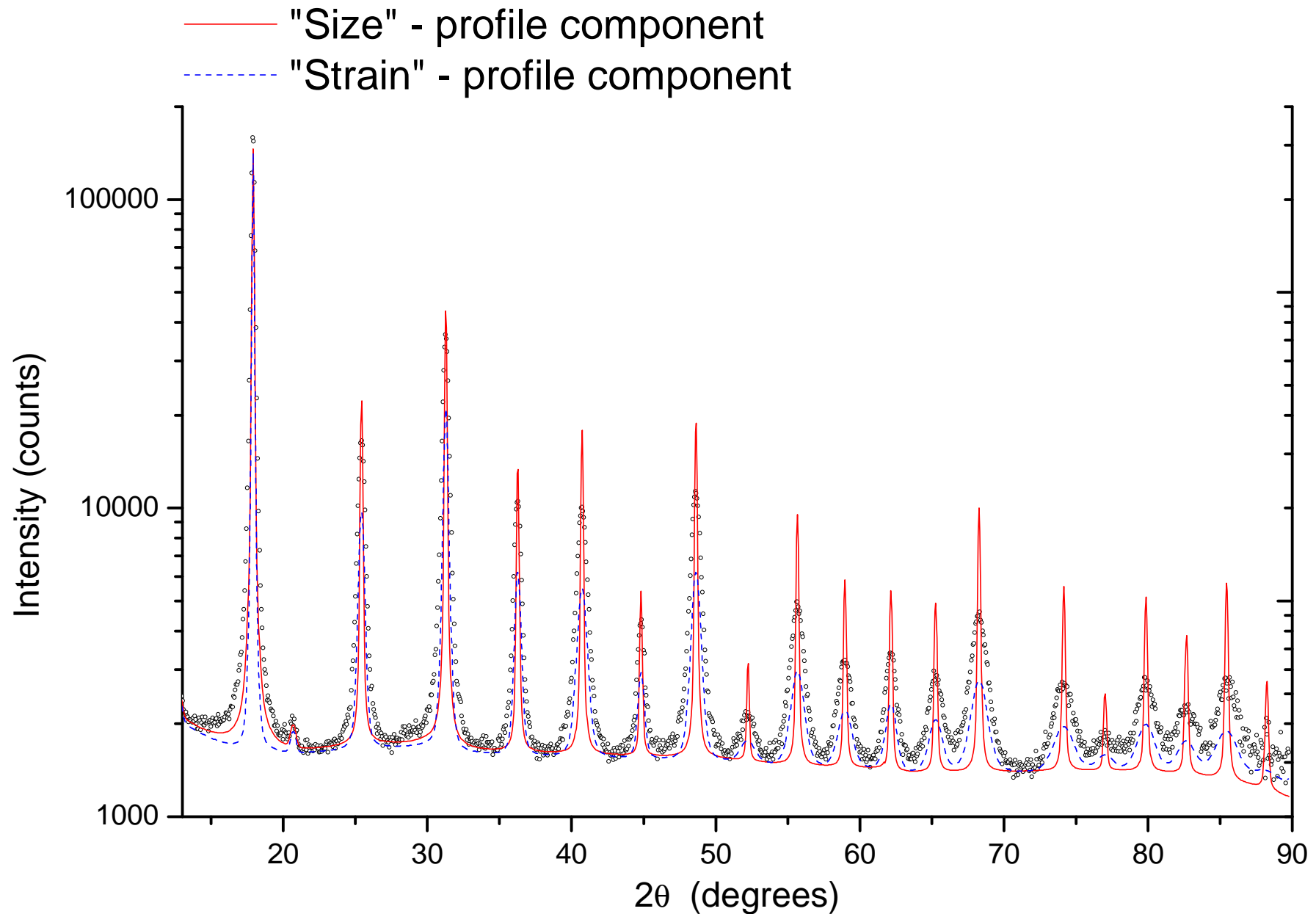
W

W

Rebuffi et al., Nat. Sci. Reports 6 20712 (2016)

NANOCRYSTALLINE Fe-1.5%Mo POWDER

Ball milled Fe1.5Mo (Fritsch P4) – data collected at ESRF – ID31 λ=0.0632 nm
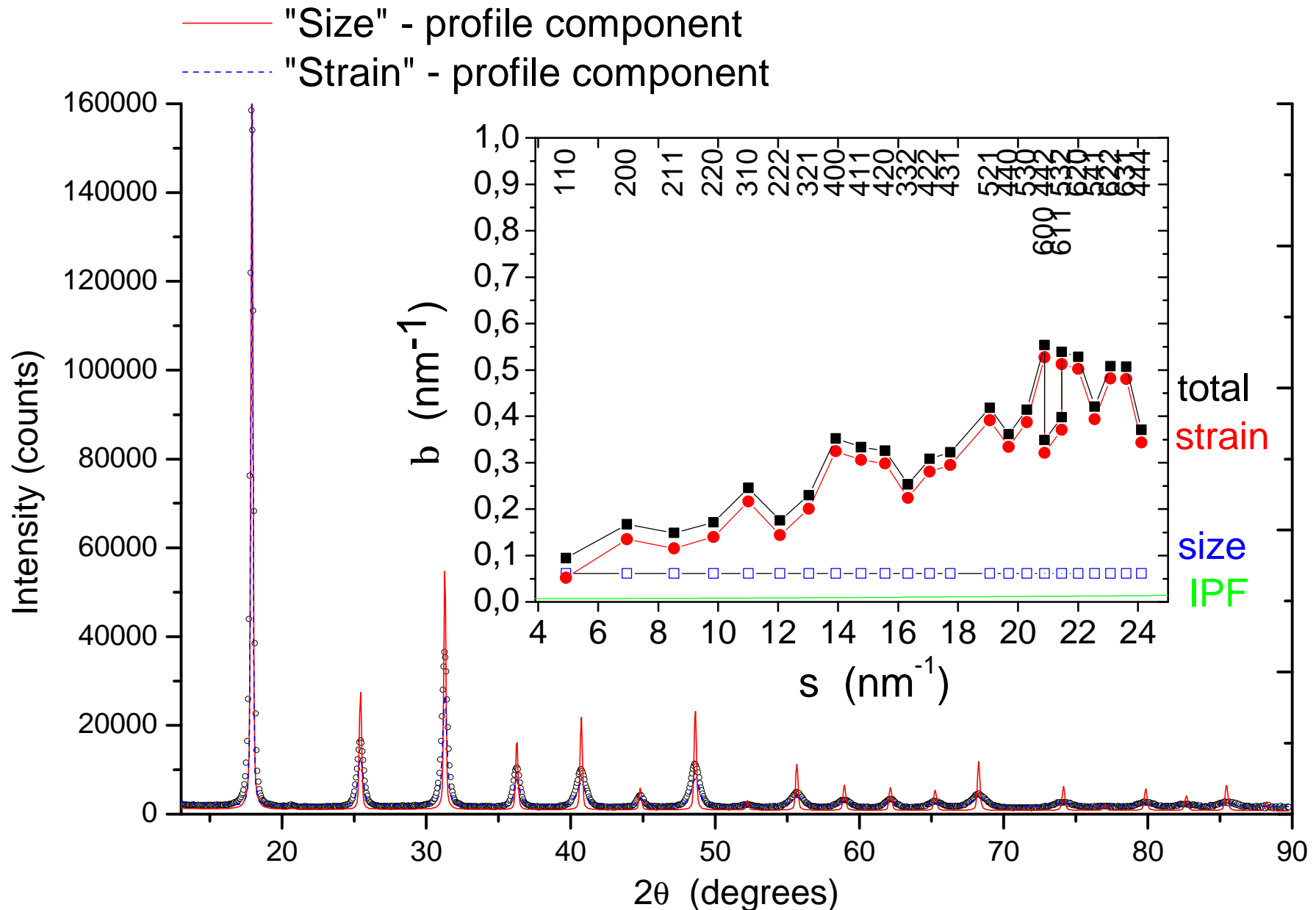
SIZE AND MICROSTRAIN PROFILE COMPONENTS
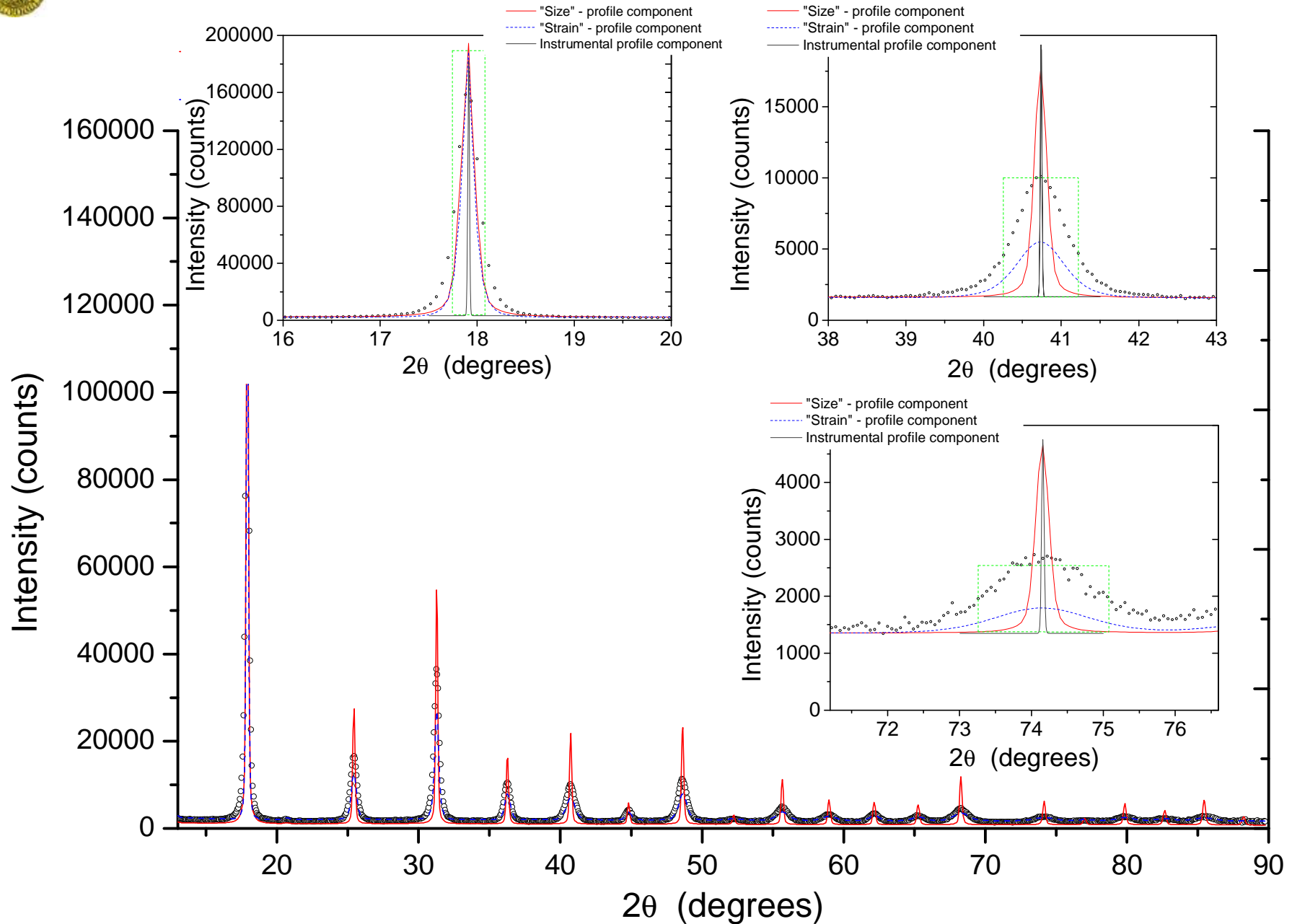
SIZE AND MICROSTRAIN PROFILE COMPONENTS

SIZE AND MICROSTRAIN PROFILE COMPONENTS

—— "Size" - profile component

------ "Strain" - profile component

Ball milled Fe1.5Mo (Fritsch P4) – data collected at ESRF – ID31 λ=0.0632 nm
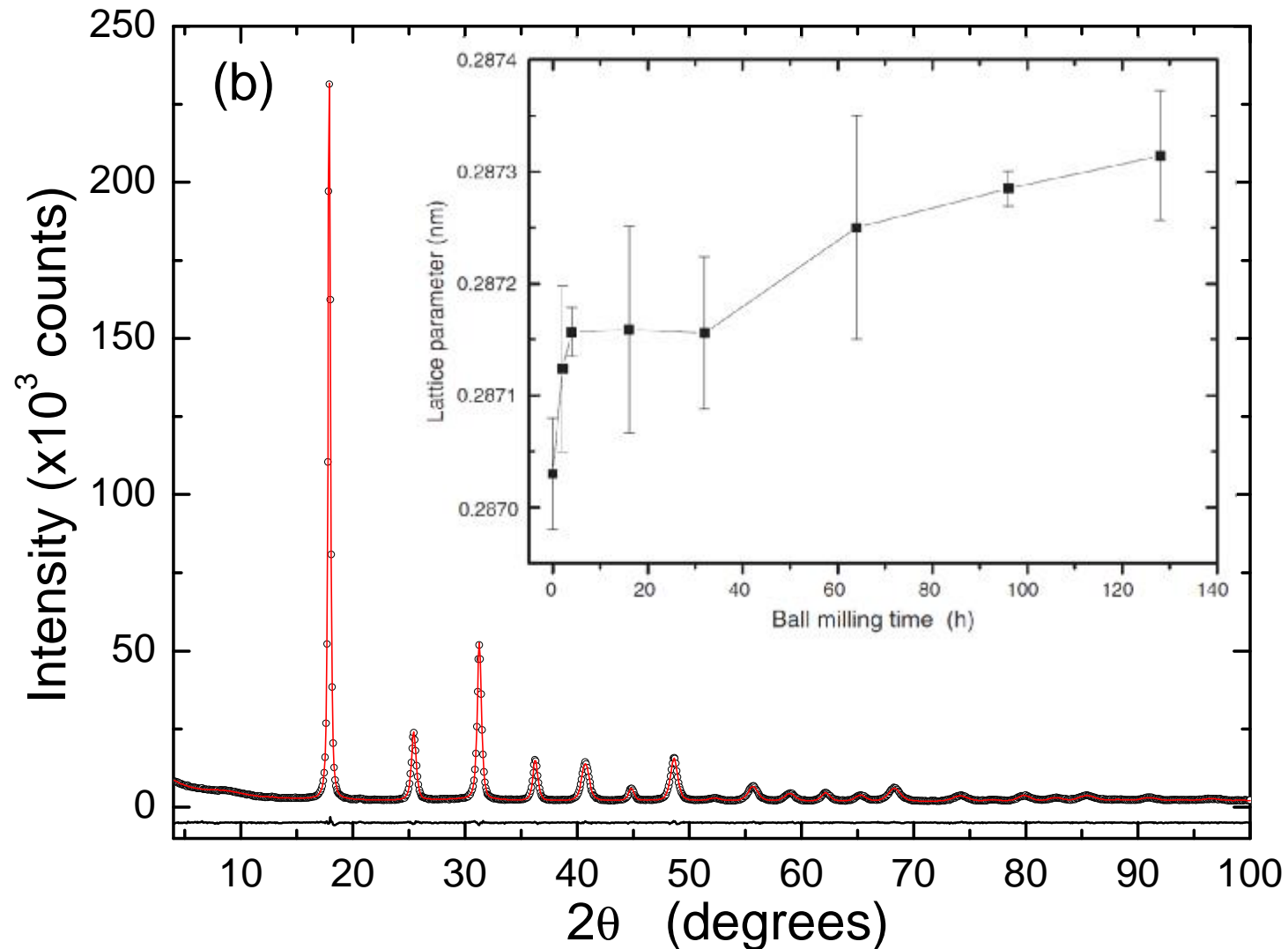
NANOCRYSTALLINE Fe-1.5%Mo POWDER

Ball milled Fe1.5Mo (Fritsch P4) – data collected at ESRF – ID31 λ=0.0632 nm
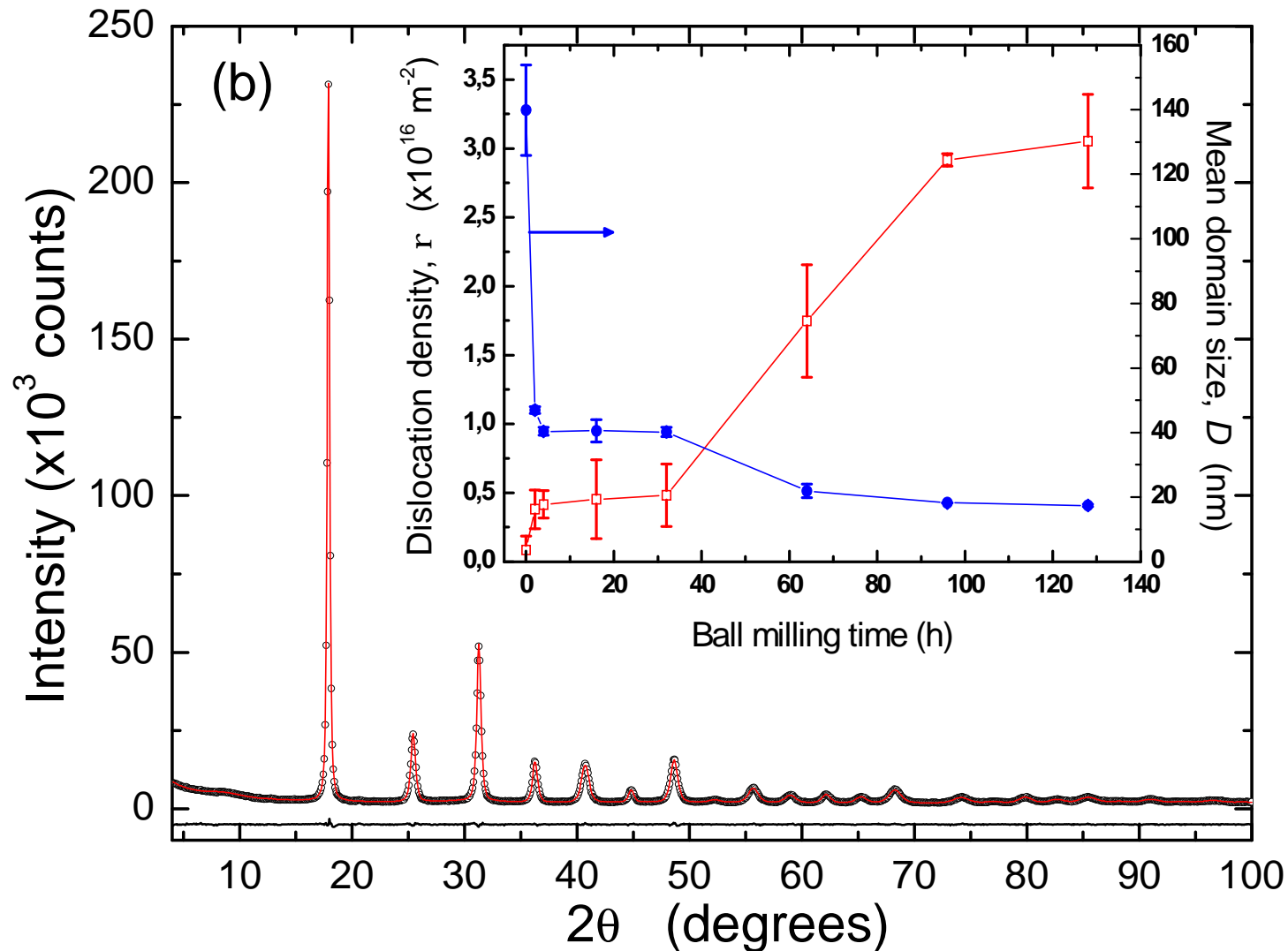
NANOCRYSTALLINE Fe-1.5%Mo POWDER

Ball milled Fe1.5Mo (Fritsch P4) – data collected at ESRF – ID31 λ=0.0632 nm
In addition to mean values, WPPM provides the size distribution
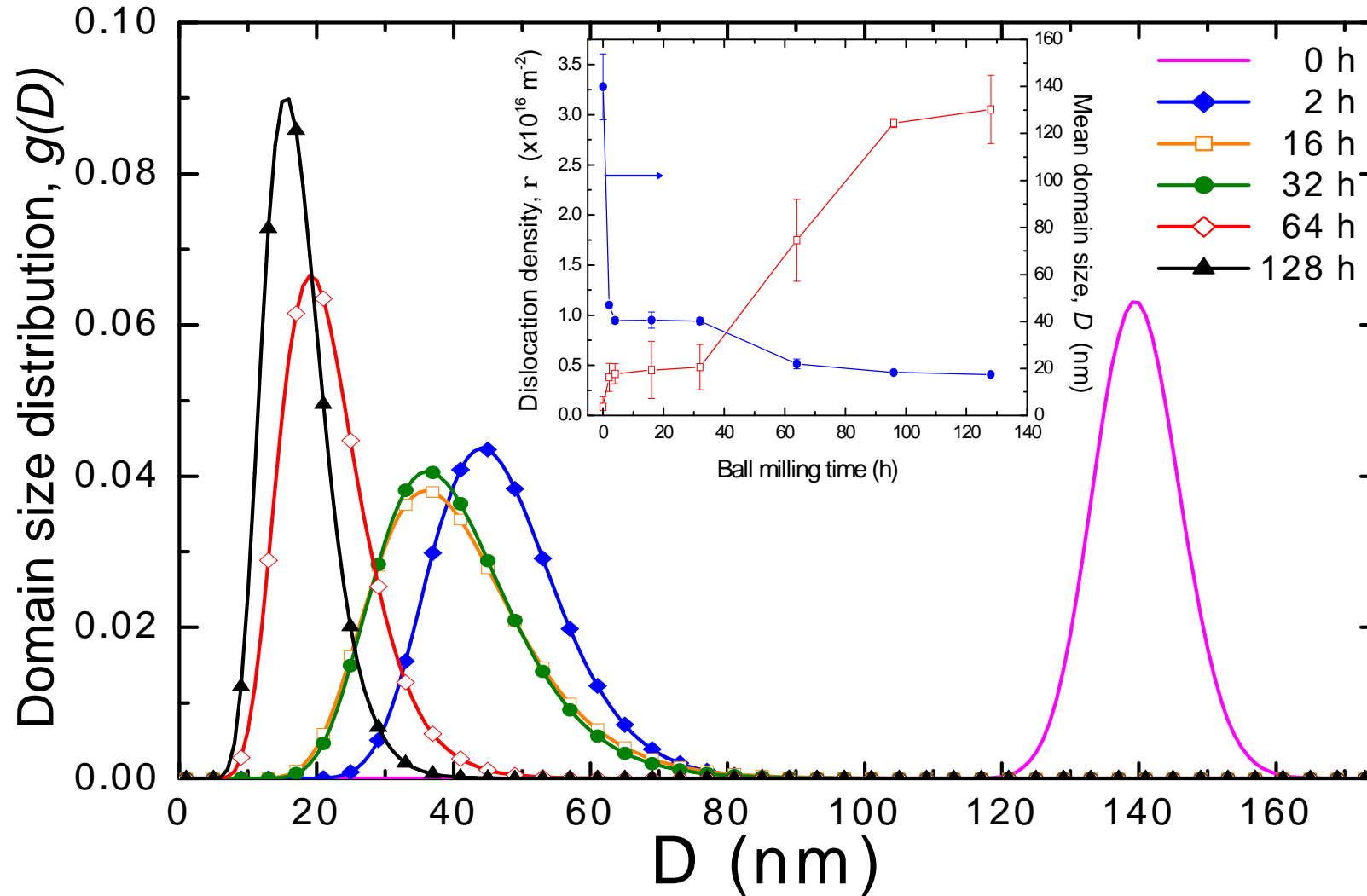
Rebuffi et al., Nat. Sci. Reports 6 20712 (2016) - open access – and references therein

CHALLENGES IN NANOTECHNOLOGY

Production of "identical" nanoparticles.   Nanocrystal size and shape:
X-ray Powder Diffraction and Transmission Electron Microscopy (TEM)

Solla Gullon et al., J. Appl. Cryst. 48 (2015) 1534
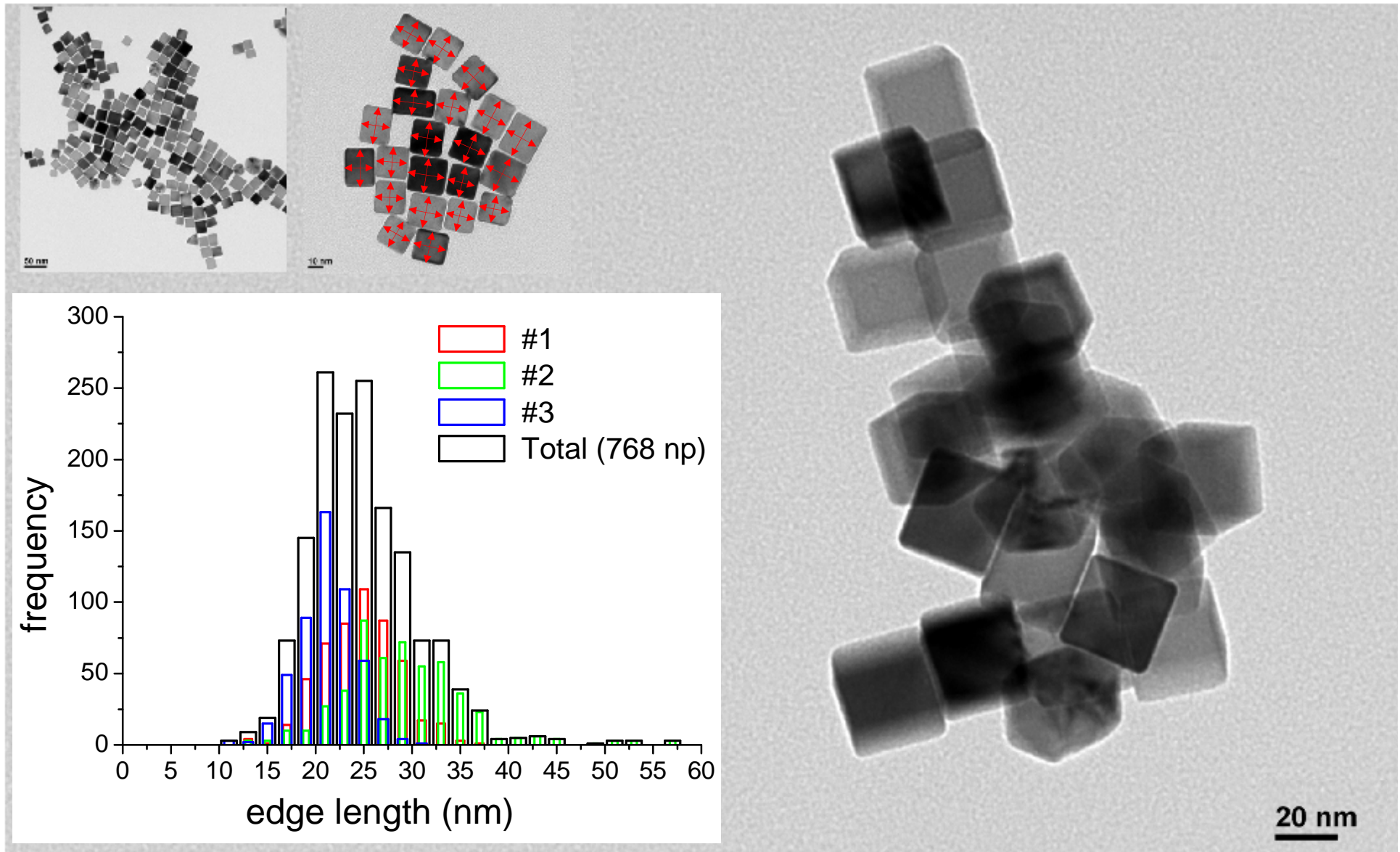
Pd nanocrystals

[110]

[111]

[100]

20 nm

{100}
{111}
{110}

P. Scardi – Diffraction from nanocrystalline materials
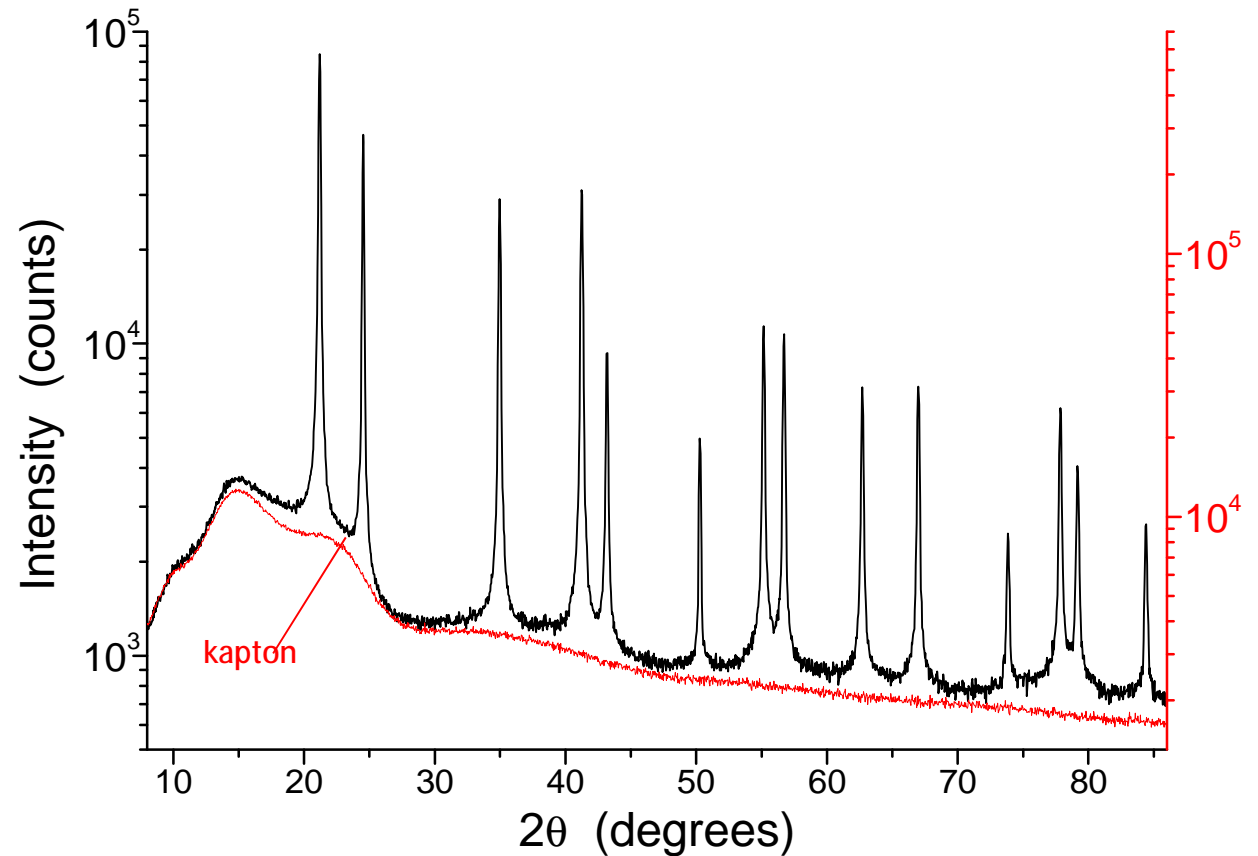
DIFFRACTION FROM NANOCRYSTALLINE *POWDER*

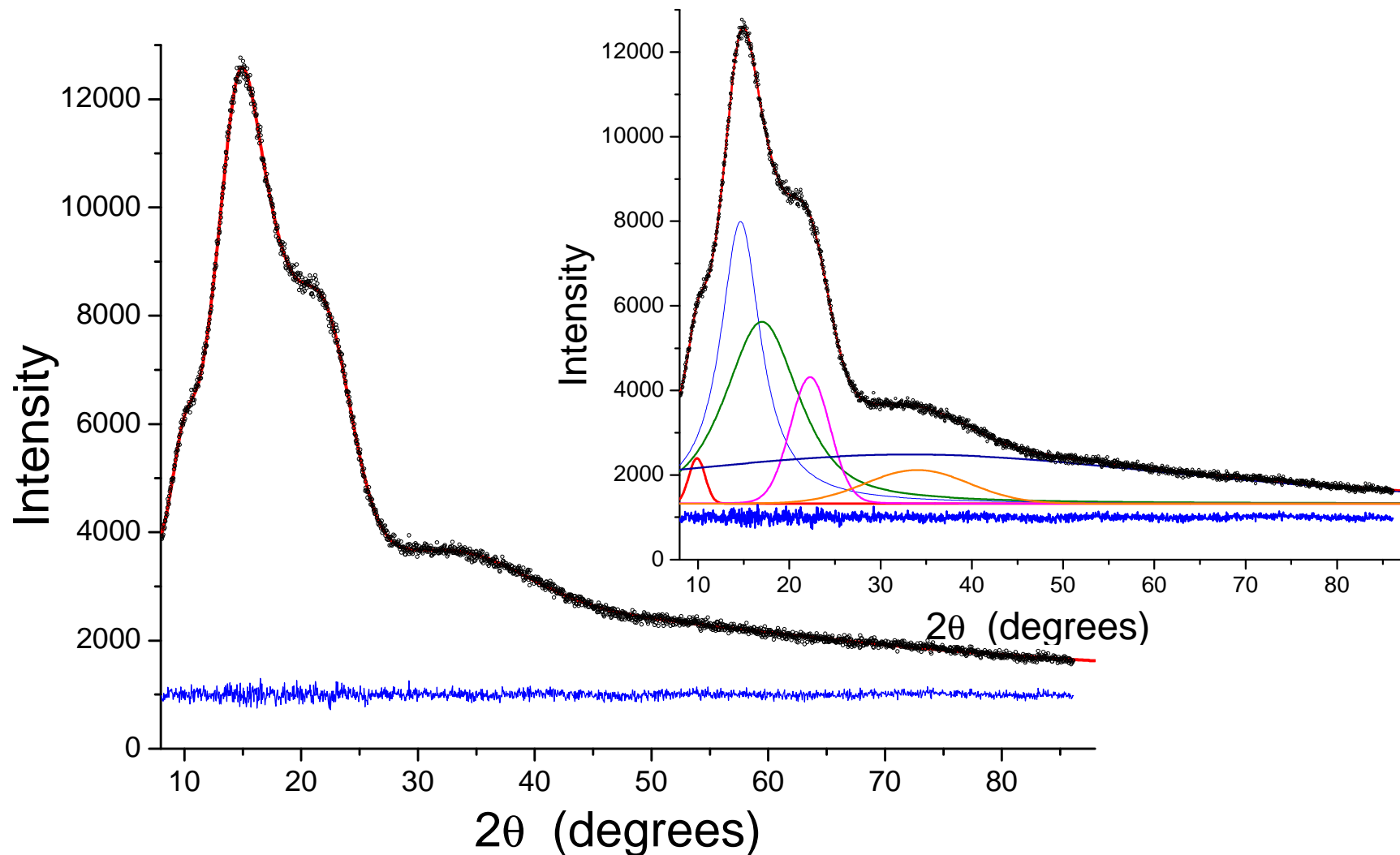# DIFFRACTION FROM NANOCRYSTALLINE *POWDER*

MCX beamline (Elettra Sincrotrone Trieste, Trieste)
Debye-Scherrer geometry , 15 keV, Ø 0.5 mm kapton capillary

Ø   Narrow instrumental profiles
Ø   Good counting statistics
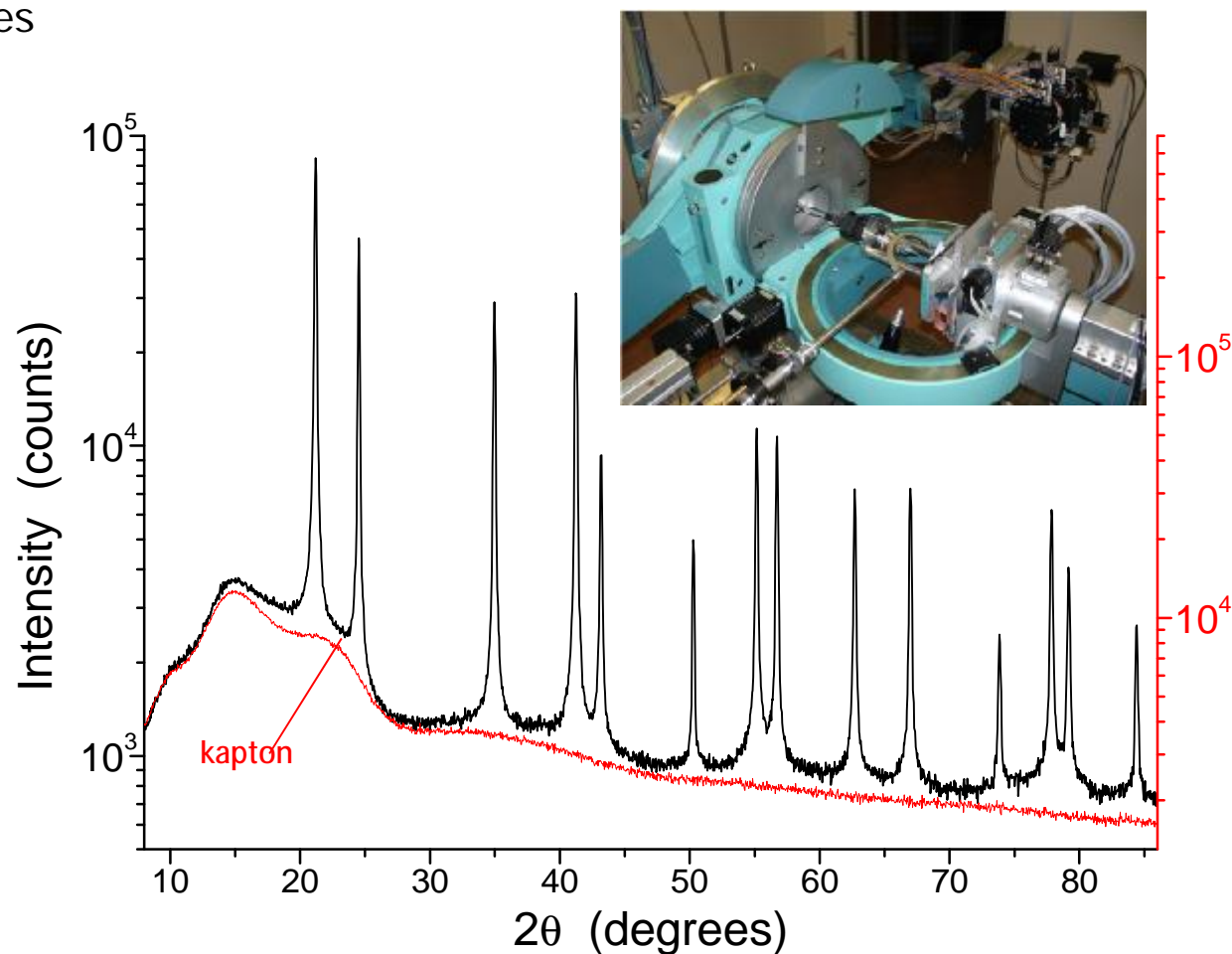
Special thanks to: M. Abdellatief, L. Rebuffi, J. Plaisier, A. Lausi

DIFFRACTION FROM NANOCRYSTALLINE *POWDER*

MCX beamline (Elettra Sincrotrone Trieste, Trieste)
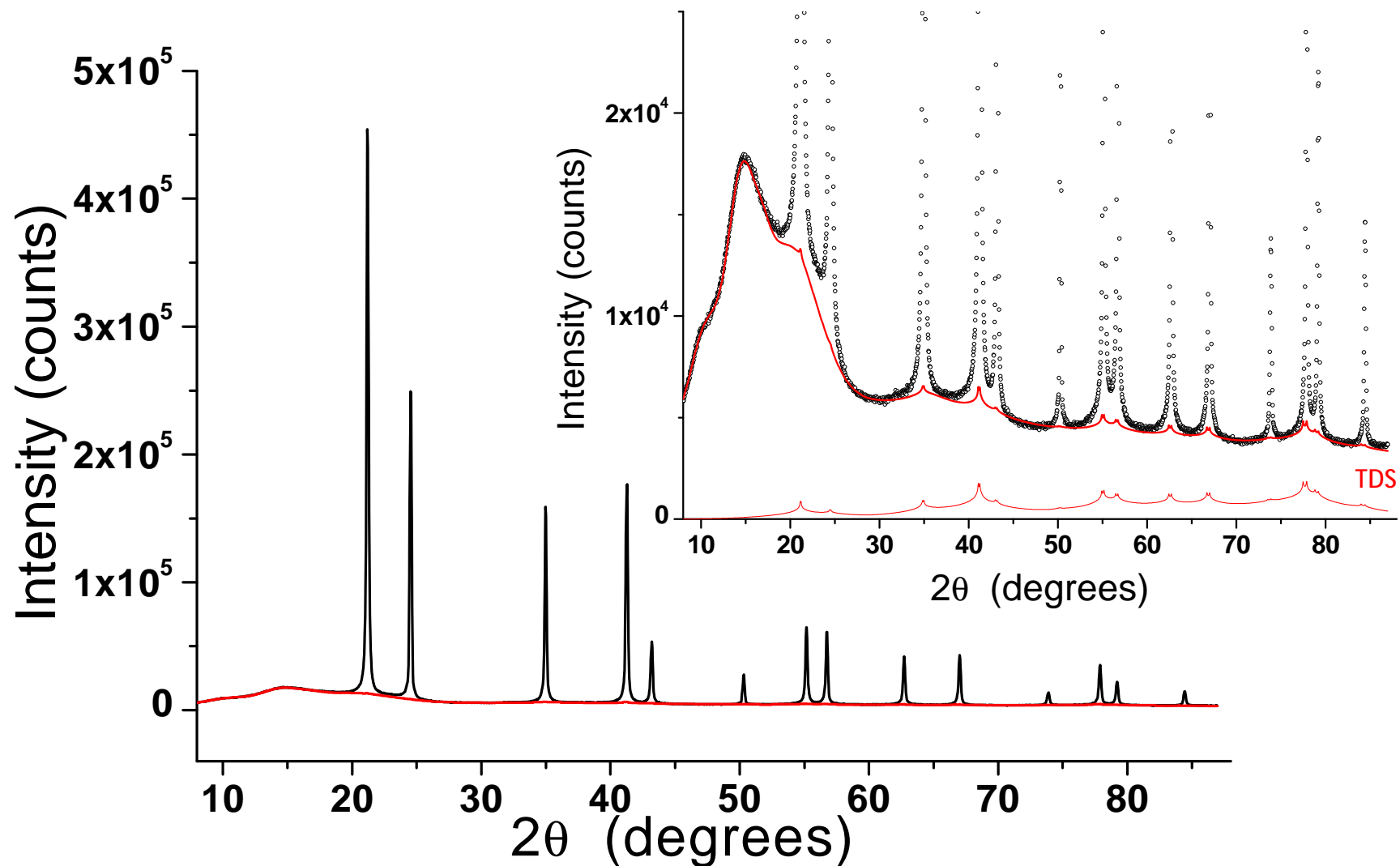Debye-Scherrer geometry , 15 keV, Ø 0.5 mm kapton capillary

Ø Negligible absorption: μ=2.71 cm^{-1} à μR≈0.07

$$A(q,R,m) = \frac{1}{pR^2} \int_0^R \int_0^{2p} \exp\left\{-m\left[\sqrt{R^2 - r^2 \sin^2(q+j)} + \sqrt{R^2 - r^2 \sin^2(q-j)}\right]\right\} \cosh\left(2mr\sin q \sin j\right) r\,dr\,dj$$
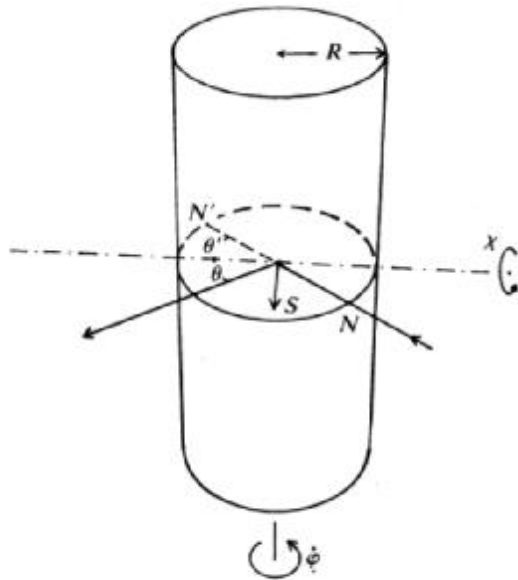
Fig. 6.3.3.1. Geometry of the Eulerian cradle with the axis of a cylindrical specimen coincident with the φ axis.
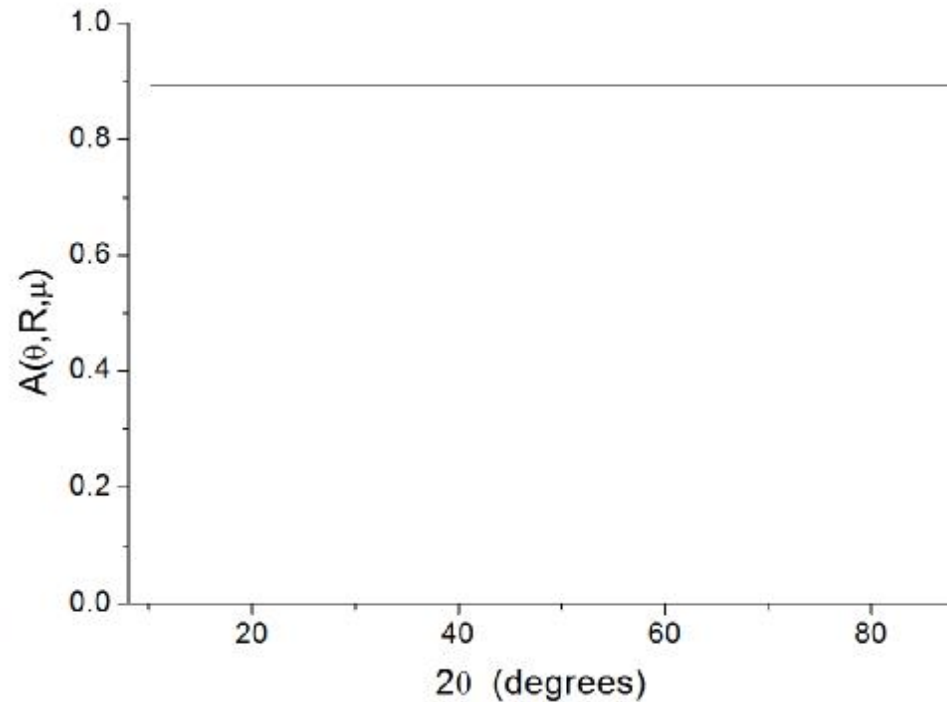
DIFFRACTION FROM NANOCRYSTALLINE *POWDER*

MCX beamline (Elettra Sincrotrone Trieste, Trieste)
Debye-Scherrer geometry , 15 keV, Ø 0.5 mm kapton capillary

Ø Carefully reproducible / controlled signal from the capillary

DIFFRACTION FROM NANOCRYSTALLINE *POWDER*

MCX beamline (Elettra Sincrotrone Trieste, Trieste)
Debye-Scherrer geometry , 15 keV, Ø 0.5 mm kapton capillary

Ø   Carefully reproducible / controlled signal from the capillary

DIFFRACTION FROM NANOCRYSTALLINE *POWDER*

Whole Powder Pattern Modelling (WPPM)

DIFFRACTION FROM NANOCRYSTALLINE *POWDER*

Whole Powder Pattern Modelling (WPPM)
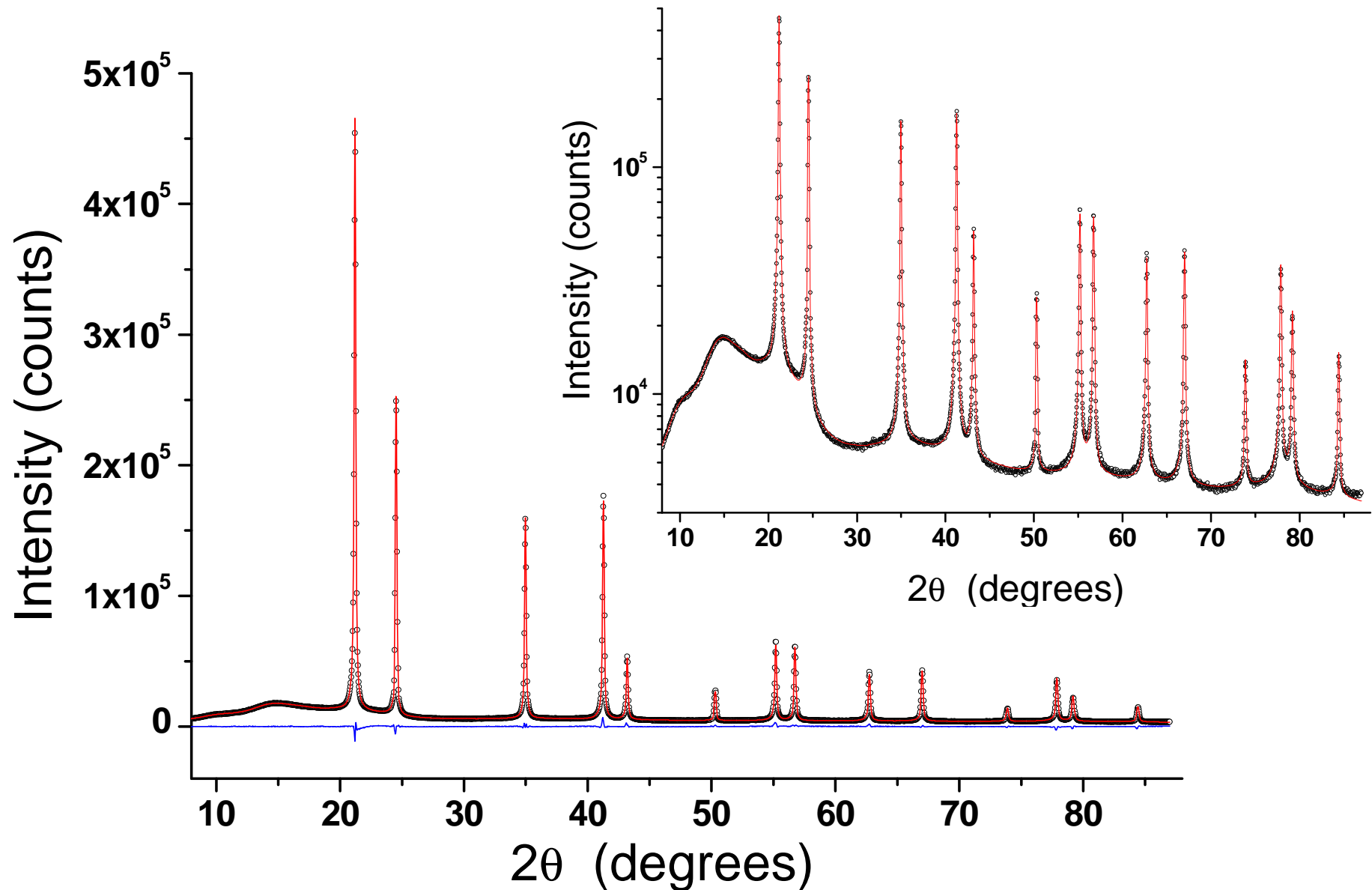
DIFFRACTION FROM NANOCRYSTALLINE *POWDER*
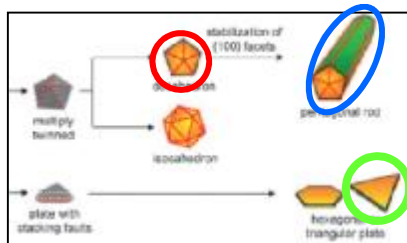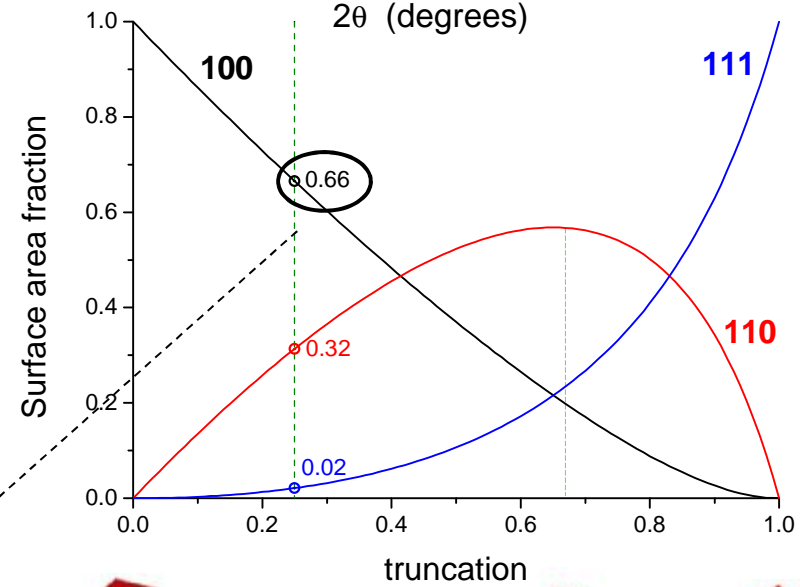
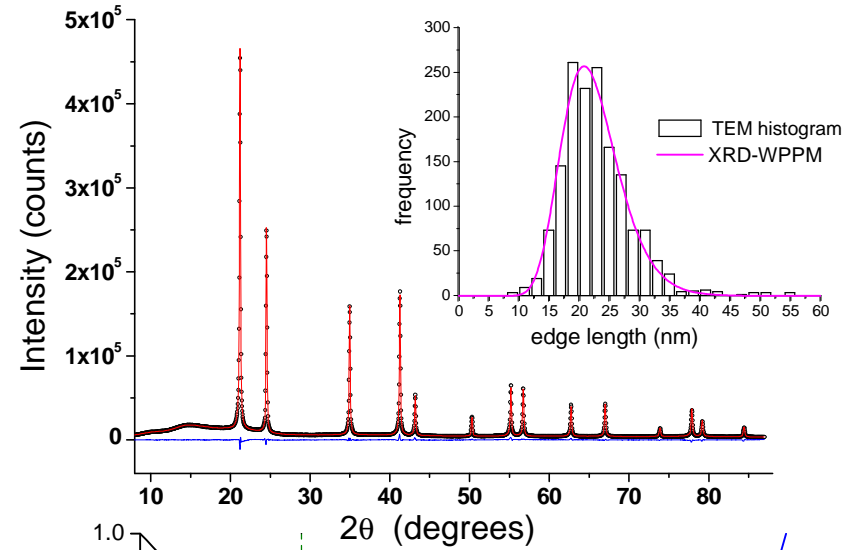lognormal distribution of cubes vs spheres: shape matters !
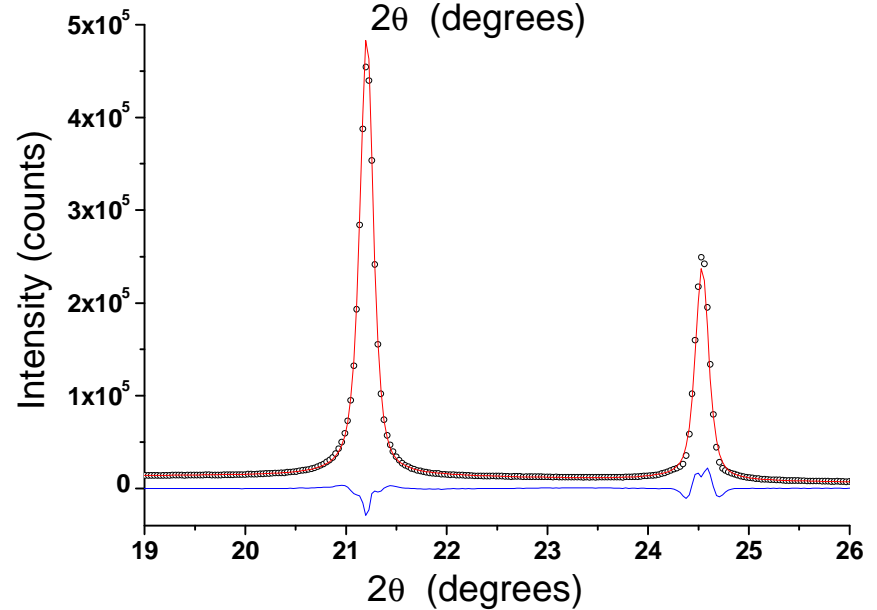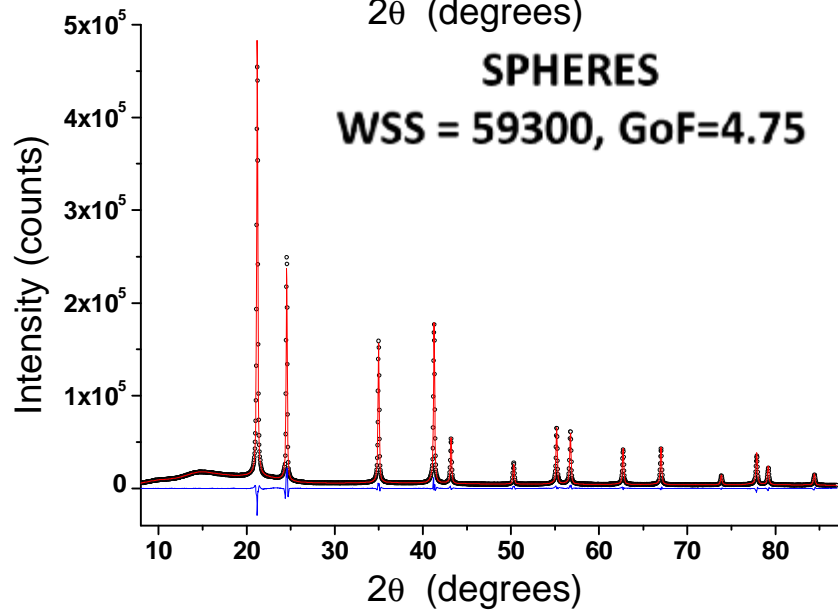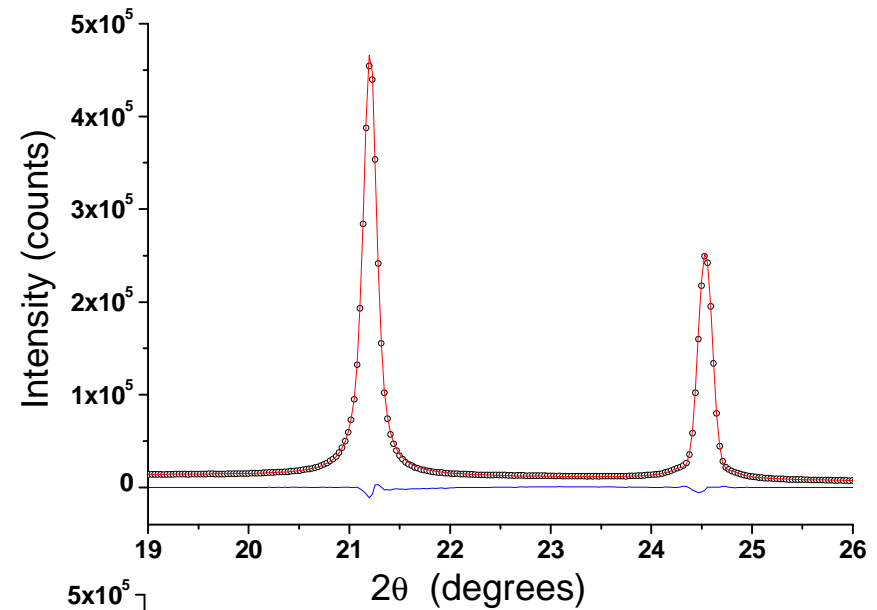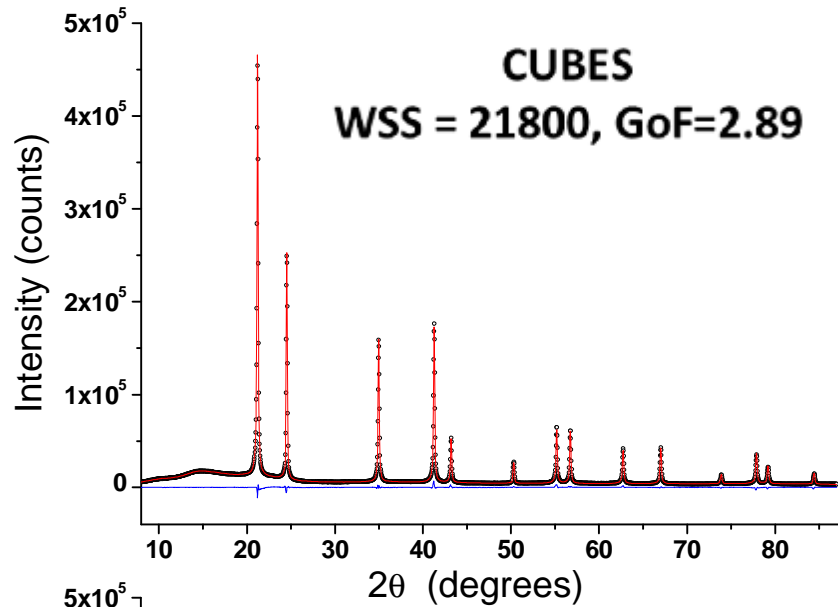
DIFFRACTION FROM NANOCRYSTALLINE *POWDER*
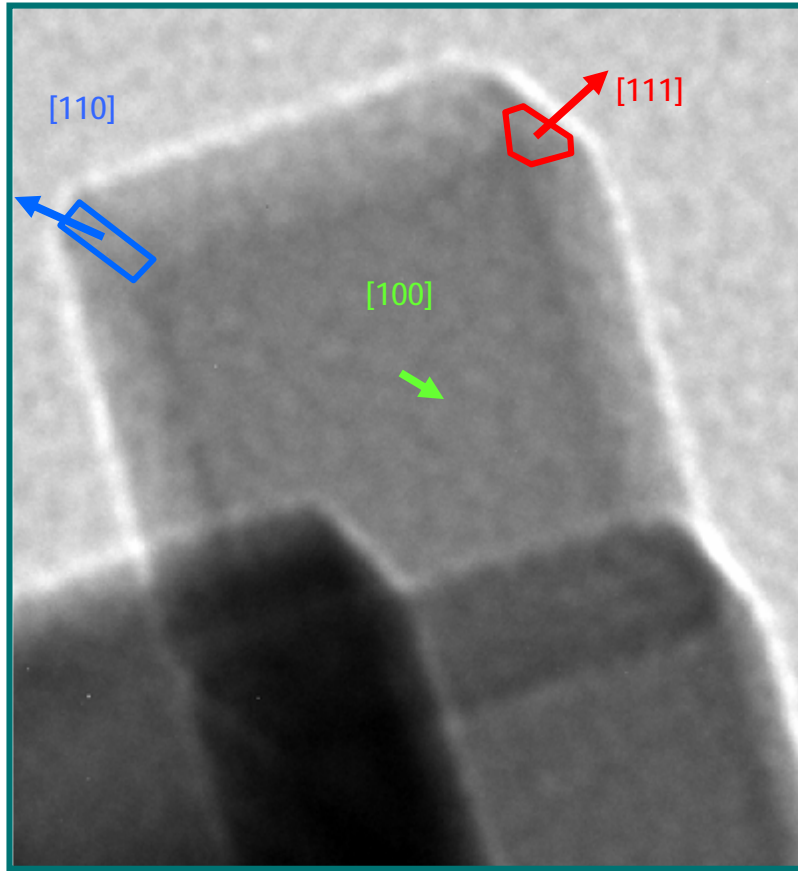
WPPM : truncated cubic Pd nanocrystal

[110]

[111]

[100]

100

111

110

0.66

0.32

0.02

Surface area fraction

truncation

Intensity (counts)

2θ (degrees)

frequency

edge length (nm)

TEM histogram
XRD-WPPM

10%

90%

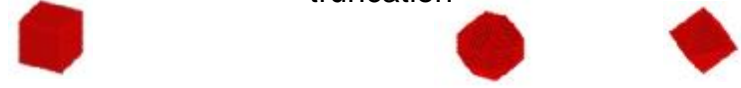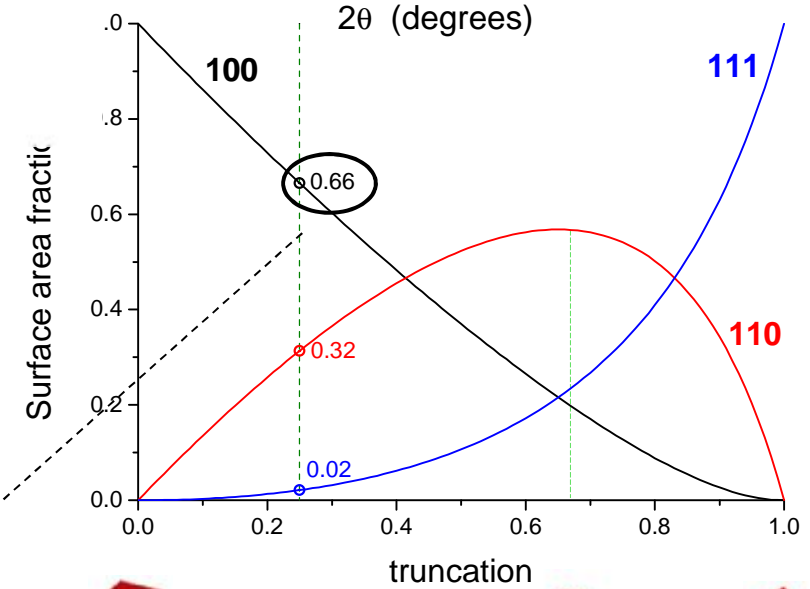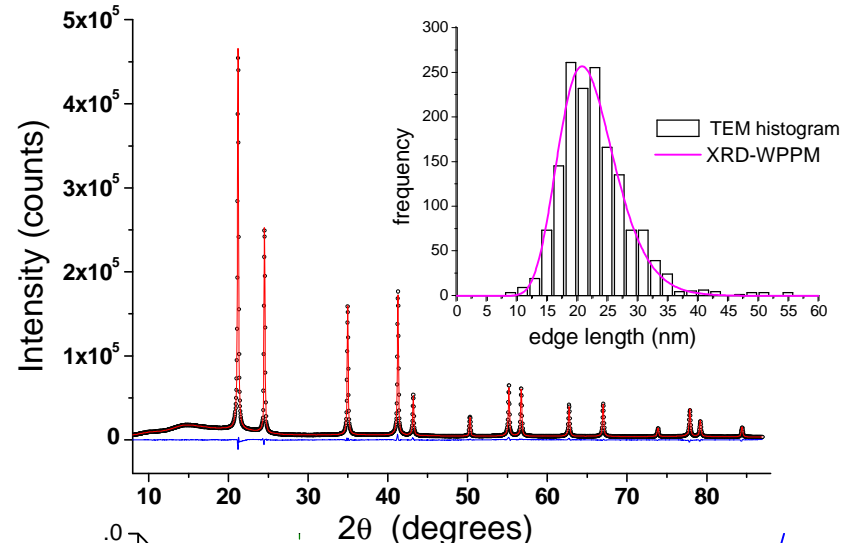# DIFFRACTION & Cu-UPD

Cu Under Potential Deposition (UPD)
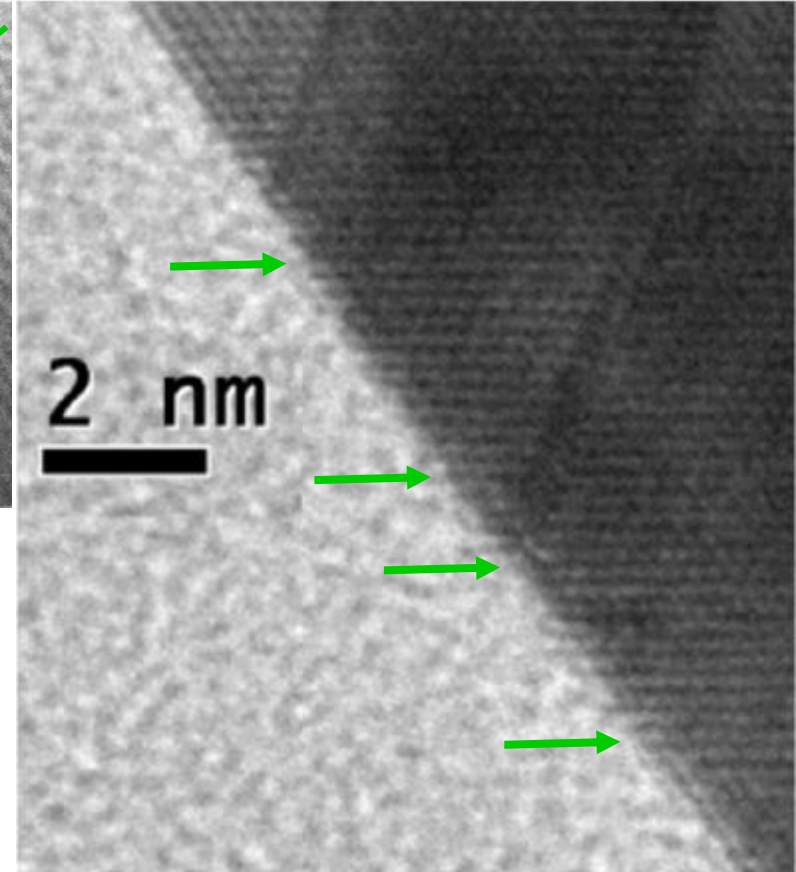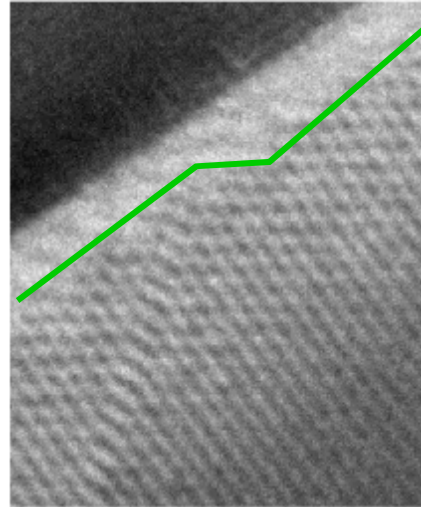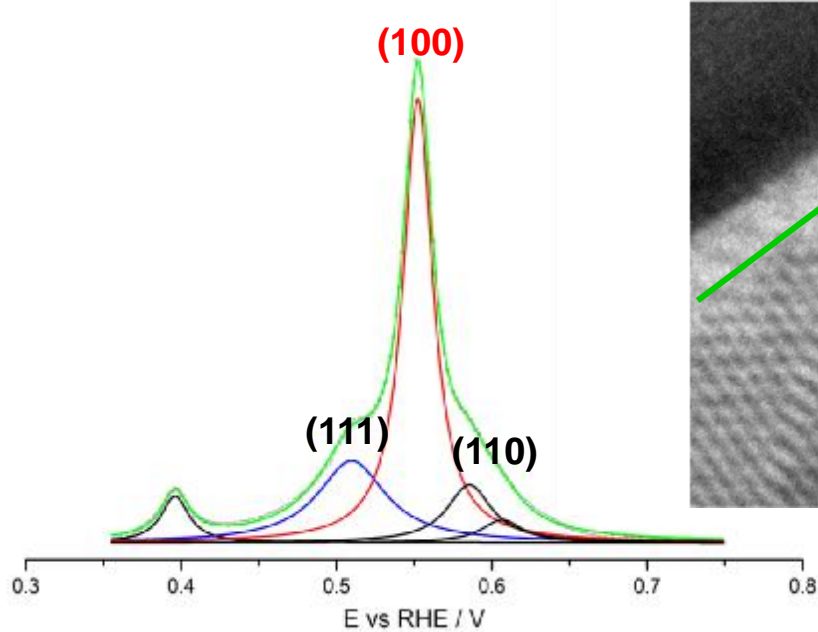
(100) area ≈ 55-60 %

(100) area: 64 %

(110) area: 28%

(111) area: 8%

10%

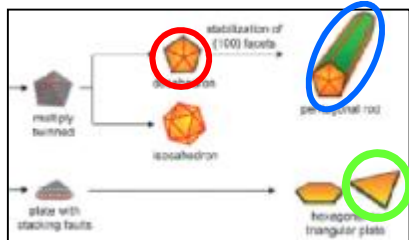## WPPM : truncated cubic Pd nanocrystal

90%

Cu Under Potential Deposition (UPD)

(100) area ≈ 55-60 %

(100) area: 64 %

»3 steps per h00 face

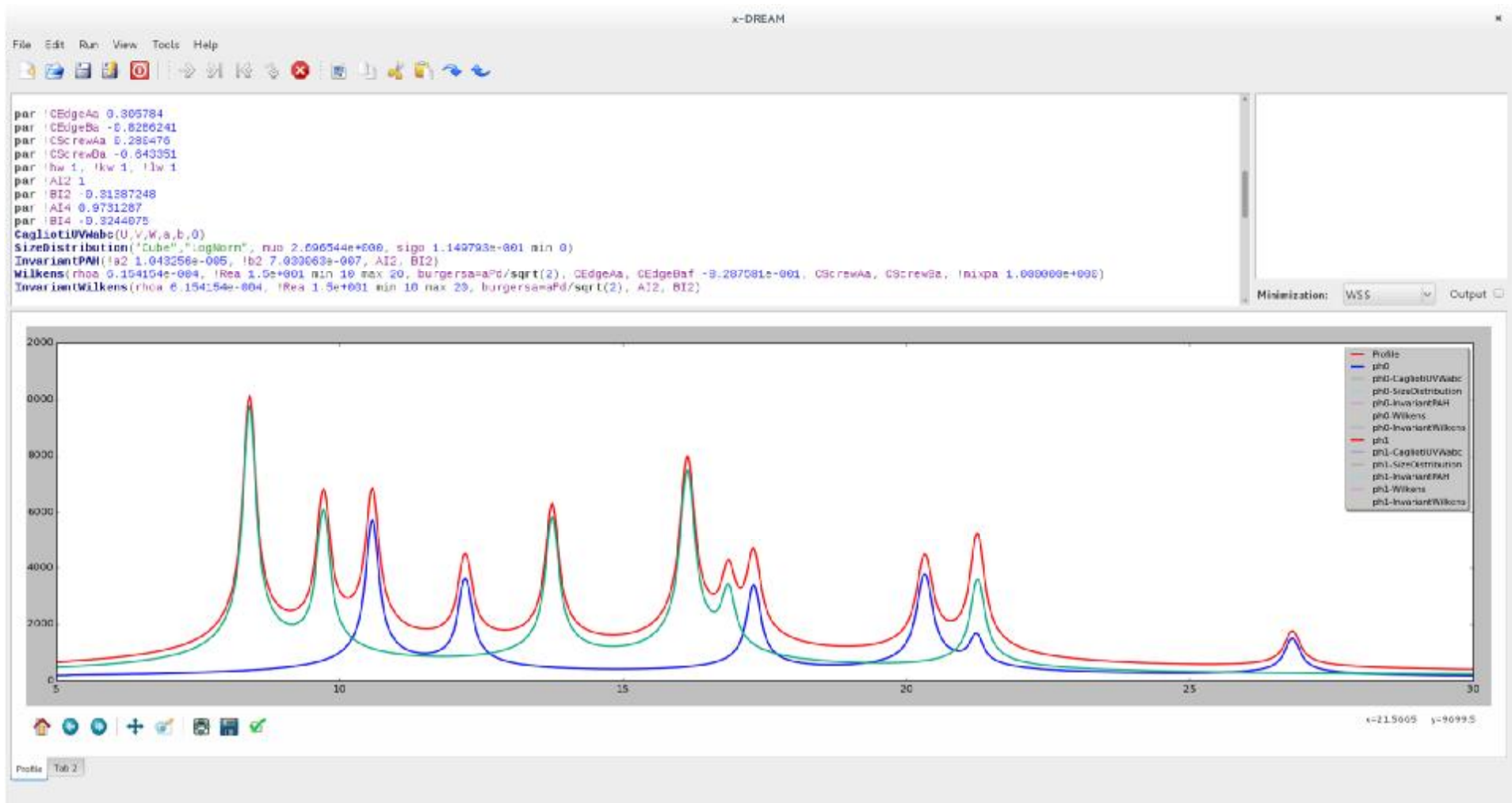(110) area: 28%

(111) area: 8%

10%

90%

WPPM SOFTWARE: *X-DREAM* EPDIC15 Bari June 2016

- Ø Open source
- Ø Multi -platform, -thread, -programming language based
- Ø Specifically designed to support learning and education